Yang *et al. Energy Mater.* **2025**, *5*, 500021
DOI: 10.20517/energymater.2024.169

Energy Materials

Review

Open Access

Insights into the role of electrolyte additives for stable Zn anodes

Shuo Yang[1,#], Yuwei Zhao[1,#], Chunyi Zhi[1,2,*]

[1]Department of Materials Science and Engineering, City University of Hong Kong, Kowloon, Hong Kong 999077, China.
[2]Center for Advanced Nuclear Safety and Sustainable Development, City University of Hong Kong, Kowloon, Hong Kong 999077, China.
[#]Authors contributed equally.

***Correspondence to:** Dr. Chunyi Zhi, Department of Materials Science and Engineering, City University of Hong Kong, 83 Tat Chee Avenue, Kowloon, Hong Kong 999077, China; Center for Advanced Nuclear Safety and Sustainable Development, City University of Hong Kong, 83 Tat Chee Avenue, Kowloon, Hong Kong 999077, China. E-mail: cy.zhi@cityu.edu.hk

How to cite this article: Yang, S.; Zhao, Y.; Zhi, C. Insights into the role of electrolyte additives for stable Zn anodes. *Energy Mater.* **2025**, *5*, 500021. https://dx.doi.org/10.20517/energymater.2024.169

Received: 12 Sep 2024 **First Decision:** 16 Oct 2024 **Revised:** 8 Nov 2024 **Accepted:** 13 Nov 2024 **Published:** 13 Jan 2025

Academic Editors: Bin Wang, Guanjie He, Jiazhao Wang **Copy Editor:** Fangling Lan **Production Editor:** Fangling Lan

Abstract

Aqueous zinc-based batteries (ZIBs), characterized by their low cost, inherent safety, and environmental sustainability, represent a promising alternative for energy storage solutions in sustainable systems. Significant advancements have been made in developing high-performance cathode materials for aqueous ZIBs, which exhibit enhanced lifespan and energy density. However, challenges associated with zinc anodes, such as dendrite formation and side reactions, impede the practical application of ZIBs. This manuscript discusses the role of electrolyte additives in the Zn electrodeposition process and comprehensively describes strategies to enhance the anode stability through additive incorporation. It specifically focuses on the underlying mechanisms that regulate the solvation structure and the electrical double layer. Finally, the manuscript concludes with future perspectives on advancing Zn anode technology, aiming to provide guidelines for developing more robust Zn-based energy storage systems.

Keywords: Aqueous batteries, zinc anode, electrolyte additive, underlying mechanism, energy storage materials

INTRODUCTION

The growing consumption of fossil fuels has prompted the necessity for sustainable energy sources, leading

to exploring alternative options with minimal environmental impact[1]. Among the various energy storage technologies, batteries, particularly lithium-ion batteries (LIBs), have emerged as the dominant choice for electric vehicles and rechargeable devices, as they provide high energy density, long cycle life, and low self-discharge[2-4]. In response to the safety concerns associated with using nonaqueous electrolytes in LIBs, researchers have been actively exploring the development of safer electrolytes and alternative battery chemistries.

Aqueous electrochemical systems hold great promise for developing next-generation batteries, offering notable advantages such as low cost, exceptional safety, and an environmentally friendly nature[5,6]. Rechargeable zinc-based batteries (ZIBs) are highly noteworthy due to the multitude of advantages associated with zinc anodes, including their abundant nature, high theoretical capacity (820 mA h g^{-1}), low electrochemical potential of (-0.763 V *vs.* the standard hydrogen electrode, SHE) and outstanding reversibility when compared to other metal anodes, such as magnesium (Mg)[7], calcium (Ca)[8], and aluminum (Al)[9], in aqueous electrolytes[10].

Despite the significant progress made in the development of high-performance cathode materials for aqueous zinc-ion batteries (ZIBs), such as V_2O_5[11], MnO_2[12], Prussian blue analogs (PBAs)[13], and organic materials[14], the commercialization of these batteries is still hampered by the limited lifespan of zinc anodes. The morphology of the electrodeposited Zn and its cycling lifespan is greatly influenced by the properties of the electrolyte and the evolution of electrical double layers (EDL)[15-17]. Electrolyte additives can adjust the electrochemical environment directly during operation, often offering a more cost-effective solution adaptable to various battery types. Therefore, the introduction of electrolyte additives has emerged as a promising and effective solution to mitigate dendrite formation and side reactions in zinc anodes, showing significant achievements, and holds great potential for further development.

This review explores the pivotal roles of electrolytes and electrodeposition processes in stabilizing Zn anodes. Subsequently, the discussion addresses the primary challenges associated with Zn anodes, including dendrite formation, hydrogen (H_2) evolution, and issues related to the durability of ZIBs. Furthermore, this manuscript elucidates strategies for enhancing the stability of Zn anodes through the strategic incorporation of additives guided by diverse mechanistic insights. The roles of representative additives are comprehensively analyzed, elucidating their stabilizing effects through regulating solvation and EDL structures. Finally, a summary and future perspectives on potential advancements in Zn anode technology through additive application are presented. This review aims to enhance the understanding of the mechanisms of additives in Zn anodes, thereby paving the way for developing more robust Zn-based energy storage systems.

INTRODUCTION OF ELECTROLYTE AND ELECTRODEPOSITION PROCESS

Electrolyte composition

The most common type in ZIBs, aqueous electrolytes, is typically composed of zinc salts [such as $ZnSO_4$, $ZnCl_2$, or $Zn(CF_3SO_3)_2$] dissolved in water. They offer high ionic conductivity, safety, and environmental friendliness. However, they tend to suffer from zinc dendrite growth, hydrogen evolution, and side reactions, which can shorten the battery lifespan. The electrolytes of ZIBs also include nonaqueous and quasi-solid-state electrolytes. When selecting an electrolyte for ZIBs, several key factors must be considered. Ionic conductivity is among the most important, directly influencing the battery's power capability. Aqueous electrolytes typically excel in ionic conductivity but must also address challenges such as dendrite formation and hydrogen evolution. The electrochemical stability window of the electrolyte is another critical consideration. It must remain stable over the battery's voltage range to avoid undesirable side

reactions. Aqueous electrolytes, for example, have a narrow voltage window of around 1.23 V due to water decomposition, often requiring additives to extend their operational range. Some additives can induce the formation of a thin, protective film on the zinc anode, which acts as a barrier to both corrosion and dendrite growth. This protective film enhances anode longevity and contributes to stable cycling performance.

The electrolyte can be categorized into two regions: the bulk electrolyte and the EDL. The bulk electrolyte refers to the region located farther away from electrode surfaces, consisting of a homogeneous solution composed of ions and solvent molecules. The composition of the bulk electrolyte can influence various physical and chemical properties, including pH, velocity, solvation structure, and ionic conductivity.

The EDL refers to the interface region between the surface of the anode and the bulk electrolyte, which plays a crucial role in determining the electrochemical properties of the system[18,19]. According to the Bockris-Devanathan-Muller (BDM) model, the EDL consists of a diffusion layer, outer Helmholtz plane (OHP), and inner Helmholtz plane (IHP) [Figure 1A and B][19-21]. In the diffusion layer, cations are surrounded by H_2O molecules, forming solvation ions, and they are randomly distributed within the layer. The IHP is composed of absorbed solvent molecules and anions. Due to the limited space within the IHP, solvated ions would disappear in this plane. Additives can influence the EDL around the zinc anode, promoting uniform ion distribution and minimizing dendrite formation.

In addition to directly measuring physical and chemical properties, the structure of the bulk electrolyte can be characterized using various techniques. Some of the most commonly used techniques include Fourier Transform Infrared Spectroscopy (FTIR), Nuclear Magnetic Resonance (NMR), and Raman Spectroscopy, which can provide valuable insights into the molecular composition, bonding, and arrangement of ions and solvent molecules in the electrolyte[22,23]. When it comes to the structure of the EDL, only a limited number of advanced characterization methods, such as time-of-flight secondary ion mass spectrometry (ToF-SIMS), can be utilized to reveal the molecular-scale dynamics of the EDL[24].

The advancement of computational simulations, particularly molecular dynamics (MD), has provided an opportunity to investigate solvation and the atomic-level structure of the EDL[25]. Figure 1C and D illustrates classical MD snapshots of the bulk electrolyte and EDL structure, respectively[26,27]. Through MD simulations, the corresponding radial distribution functions (RDFs) and coordination numbers (CN) of various ion pairs (e.g., Zn^{2+} and SO_4^{2-}) can be calculated, providing insights into the first solvation shell of Zn^{2+}. This information is instrumental in explaining the dynamics of ionic conductivity, variations in water coordination, the formation of the solid electrolyte interphase (SEI) in aqueous ZIBs, and other related phenomena. Furthermore, the spatial distribution of solvent molecules and ions along the vertical electrode surface can offer detailed information about the structure of IHP and OHP [Figure 1E][27]. In addition to classical MD simulations, incorporating recently developed techniques such as ab initio molecular dynamics (AIMD) and machine-learning MD enables the study of charge transfer processes, including bond breaking and bond forming, while considering the polarization effects[28].

Additives play a key role in shaping the physical and chemical properties of bulk electrolyte properties, including pH, velocity, solvation structure, and ionic conductivity. At the EDL - the interface between the electrode and electrolyte - additives further influence ion adsorption, charge distribution, and the local electric field. In this interfacial region, additives can encourage uniform zinc ion deposition by balancing the electric field and charge density, which helps reduce dendrite formation and improves electrode stability.

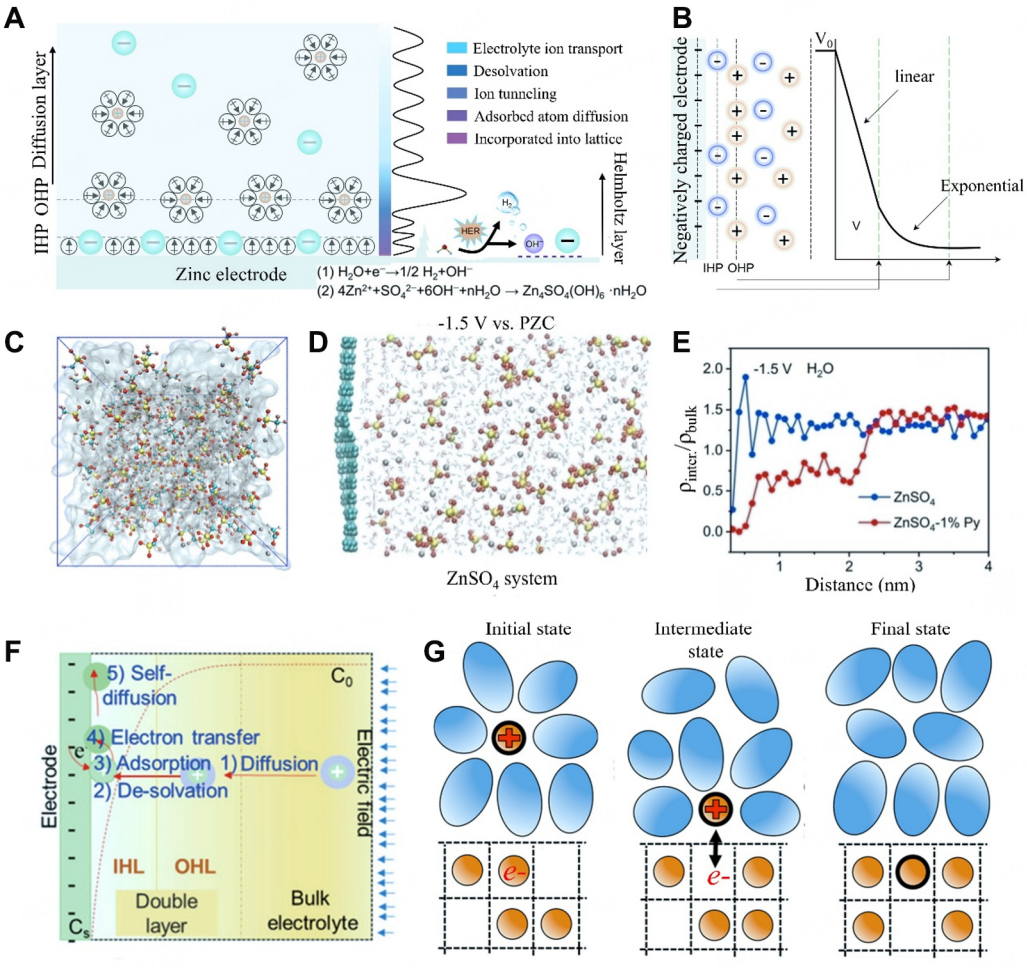

Figure 1. Electrolyte composition and the electrodeposition process. (A) Schematic illustrations of the EDL structure for Zn electrode in $ZnSO_4$ aqueous system. (B) Gouty-Chapman-Stern model depicting the EDL structure[19]. Copyright 2023 Elsevier B.V. (C) MD snapshots showing the electrolyte containing 2 M $Zn(OTF)_2$ and 0.7 M CH_3COO^-[26]. Copyright 2024 The Royal Society of Chemistry. (D) MD snapshots showing the EDL structure of $ZnSO_4$ electrolyte. (E) Spatial solvent molecule and ion distribution along the vertical electrode surface for different electrolytes[27]. Copyright 2023 John Wiley & Sons. (F) Illustration of the typical electrodeposition process[29]. Copyright 2022 John Wiley & Sons. (G) Illustration of the charge transfer process[30]. Copyright 2013 The American Chemical Society.

Additive concentration is crucial in shaping the solvation structure of ions. At lower concentrations, additives may partially modify the solvation shell, while at higher concentrations, they can establish a more stable solvation environment that resists unwanted side reactions, such as hydrogen evolution. Depending on the concentration, additives can either promote or inhibit ion pairing between zinc ions and anions, influencing ion transport dynamics. Also, at higher concentrations, additives can alter the ionic composition near the electrode surface, redistributing ions in the EDL. This redistribution affects the deposition and stripping of zinc ions during charge and discharge cycles; optimal concentrations encourage uniform deposition by smoothing the electric field across the electrode surface. Furthermore, electrical conductivity typically increases with additive concentration initially but then begins to decrease beyond a certain point. However, excessive concentrations may elevate viscosity, hindering ion mobility. Additionally, the choice of additive concentration affects the battery's overall cost and environmental impact, making it essential to balance performance gains with sustainable practices.

ELECTRODEPOSITION PROCESS

The electrodeposition of metals involves a series of sequential steps, including diffusion, adsorption, desolvation, electron transfer, and self-diffusion [Figure 1F][29]. Initially, the solvated metal ions from the bulk electrolyte would migrate towards the electrode substrate through diffusion and subsequently be absorbed on the OHP. Following this, the solvated ions undergo a gradual desolvation process, transforming into desolvated ions, which then transport to the IHP. Once the desolvated metal ions reach the IHP, the desolvated metal ions may gain electrons from the electrode, reducing the desolvated metal ions and the subsequent formation of metal atoms. Finally, metal atoms migrate along the substrate surface, forming strong chemical bonds at active sites, and then enter the crystal lattice[30].

Another extensively studied theory in electrodeposition is the Marcus-Hush model, which proposes that the reduction of metal ions occurs through an outer-sphere electron transfer reaction within the EDL structure[31]. According to this theory, the electron transfer initially occurs to the solvated cations in the outer sphere, reducing these cations into metal atoms that subsequently adsorb onto the metal surface. In this process, the solvated ions do not need to cross the interface, although their distance from the metal surface may vary slightly[32-36].

However, recent studies have revealed that the removal of the solvation shell and the reduction of effective charge on metal ions occur through numerous small steps involving a mechanism of formation followed by rupture[37]. When both mass and charge cross the interface, the charge must be carried by the ion species rather than electrons due to the significant difference in timescales for electron and ion transfer[33]. As the electrons transfer to the solvated cations, the solvation structure of the cations concurrently undergoes reorganization to lower the system's energy [Figure 1G][30,38]. The solvated cations with lower valency ultimately traverse the double layer and are reduced to metal atoms.

CHALLENGES OF ZN ANODES

Significant advancements have been made in ZIBs. However, several challenges still impede their widespread application, particularly concerning the limited lifespan and low utilization efficiency of zinc anodes[39]. In addition to addressing the cycling stability of ZIBs, it is crucial to consider the overall durability of these batteries. Durability refers to their ability to maintain reliability under various operating conditions, including calendar aging and overcharging, which is vital for practical implementation[5,40,41]. In this section, we will focus on discussing the challenges related to the stability of the Zn anode and the overall durability of ZIBs.

Dendrite formation

The fundamental cause of dendrite formation is primarily attributed to the slower mass transfer kinetics compared to the rapid electrochemical reduction rate[31]. The ideal scenario would involve consistent mass transfer of metal cations throughout the electrode surface to achieve uniform metal electrodeposition. However, in practical situations, the movement of metal cations is influenced by various factors, including diffusion, convection, and migration, leading to complex mass transfer phenomena [Figure 2A][42].

As depicted in Figure 2B, prior to the deposition of metal ions, the cations migrate from the bulk electrolyte towards the vicinity of the electrode[43,44]. The diffusion coefficient influences the migration rate of metal ions, while the electrochemical reduction rate is determined by the faradaic current density, as given in the Butler-Volmer equation:[31]

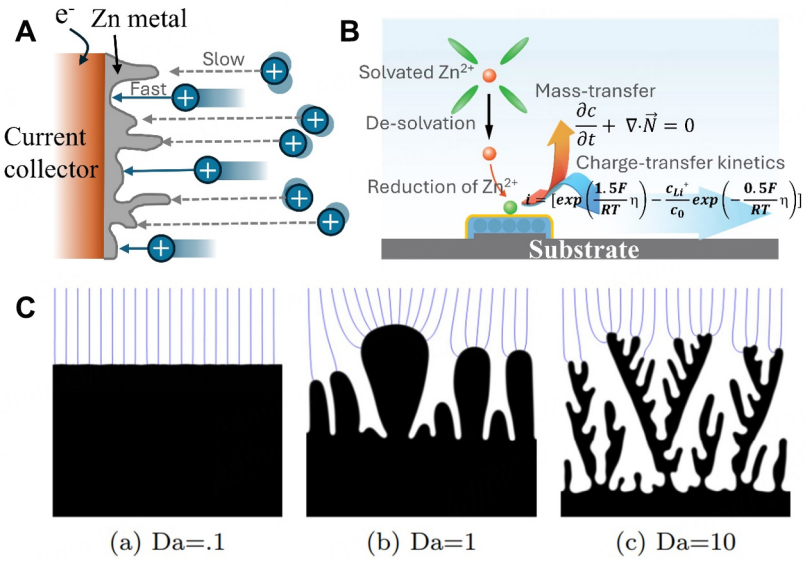

Figure 2. Dendrite formation in the liquid electrolytes. (A) Schematic illustrations of the movement of metal cations with different speeds under complex mass transfer, including diffusion, convection, and migration. (B) Schematic diagram of Zn electrodeposition model combining mass-transfer and charge-transfer kinetics. (C) Effects of dimensionless Damkohler numbers on electrodeposition morphology[44]. Copyright 2015 The American Physical Society.

$$J = J_0[e^{-\alpha nf\eta} - e^{(1-\alpha)nf\eta}] \quad (1)$$

where J_0 represents the exchange current density, α denotes the transfer coefficient, n stands for the number of electrons transferred, f is the inverse of the thermal voltage, and η indicates the overpotential.

In general, the migration rate of metal ions is significantly slower than the electrochemical reduction rate, particularly in situations with a "tip effect", leading to a higher electric field intensity and faster reaction kinetics[45]. This rate imbalance results in the formation of strong concentration gradients on the zinc ion surface, ultimately leading to dendrite growth. Consequently, based on Equation (1), a lower J_0 value would result in slower electroreduction kinetics, thus alleviating the conflict between mass transfer and charge transfer. This, in turn, promotes the formation of dendrite-free morphologies.

Another valuable model for quantifying the relationship between mass transfer and charge transfer is through using a dimensionless Damkohler number, expressed as:

$$D_a = \frac{J_0 V_m}{nFD/L} \quad (2)$$

where J_0 represents the exchange current density, n denotes the number of electrons transferred, D indicates the mutual diffusion coefficient of the electrolyte, and L points to the distance between the two electrodes[44].

According to phase-field modeling, when the value of the Damkohler number is 0.1, it indicates fast diffusion compared to the electrode reaction rate [Figure 2C]. This condition promotes the formation of a flat deposition morphology in a 1 M zinc sulfate ($ZnSO_4$) electrolyte. When the Damkohler number is greater than 1, dendrite formation on the surface of the zinc anode is observed due to the slow diffusion of Zn^{2+} ions in the electrolyte. The findings suggest that modifying the electrolyte to decrease the

electrochemical reaction rate could be a successful strategy for controlling dendrite growth.

H_2 evolution

The driving force behind the evolution of H_2 is the thermodynamic instability of the zinc anode when exposed to an aqueous solution. The hydrogen evolution potential in the neutral aqueous electrolyte (-0.41 V *vs.* SHE) is higher than the potential for Zn deposition, indicating a tendency for hydrogen production in the electrolyte[46]. Furthermore, the corrosion of the Zn anode in a weak acid electrolyte can also contribute to generating H_2 gas.

The hydrogen evolution can be directly observed using an *in-situ* optical microscope, where small bubbles can be seen on the surface of the zinc anode after a certain deposition time in 1 M zinc bis(trifluoromethanesulfonyl)imide [$Zn(TFSI)_2$] electrolyte [Figure 3A][47]. Similar phenomena have also been observed in other commonly used electrolytes, such as 1 M $ZnSO_4$ and 3 M zinc bis(trifluoromethanesulfonate) [$Zn(OTF)_2$] electrolytes[16]. Notably, using commonly employed electrolytes with a weak acid nature can induce a reaction with the Zn anode. The reaction would lead to the generation of H_2 gas under open circuit potential (OCP) conditions in addition to the H_2 production induced by electrochemical processes, as demonstrated by the online differential electrochemical mass spectrometry (DEMS) analysis [Figure 3B][47].

Besides the online DEMS technique, which allows for direct characterization of the relative amount of H_2 during the electrochemical process, *in-situ* measurements can also be performed by connecting the batteries to a gas chromatograph (GC)[48]. This method enables qualitative assessment of the hydrogen content in different electrolyte systems [Figure 3C and D]. An *in-situ* gas pressure detector was employed to quantify the H_2 generated during the deposition process. This detector allowed for the measurement of gas evolution within the designed cell[49]. As shown in Figure 3E, the battery's pressure displayed an increasing trend following the deposition of Zn, which could then be converted into the corresponding amount of H_2 involved in the reaction process, utilizing the ideal gas equation.

The generation of H_2 gas during the electrochemical process can significantly influence the coulombic efficiency (CE) of the batteries, owing to the reduced reversibility of the Zn anode and the consumption of a portion of the charge. As a result, the overall efficiency of the batteries is compromised. Additionally, the generation of H_2 gas from the decomposition of the electrolyte can lead to an increase in the pH values of the electrolyte, particularly at the interfaces between the electrolyte and the electrodes [Figure 3F][50]. Consequently, a passive layer on the surface of the Zn anode occurs, resulting in a reduced utilization rate of Zn [Figure 3G].

Challenges related to the durability of ZIBs

The durability of ZIBs refers to their ability to maintain reliable performance under diverse operating conditions, including fluctuations in temperature, humidity, overcharge scenarios, and calendar aging conditions[51]. The research on ZIBs has primarily prioritized prolonging the cycling lifespan, with limited attention and understanding given to the durability.

Calendar aging conditions, extensively investigated in relation to battery durability, primarily cause capacity deterioration due to degradation of the Zn anode. Figure 4A-F displays the scanning electron microscopy (SEM) and transmission electron microscopy (TEM) images of the Zn anode before and after 24 h of aging. These provide visual evidence that can help elucidate the underlying causes of capacity degradation in ZIBs during calendar aging[52]. The Cu current collector surface appears free of residual Zn after stripping before

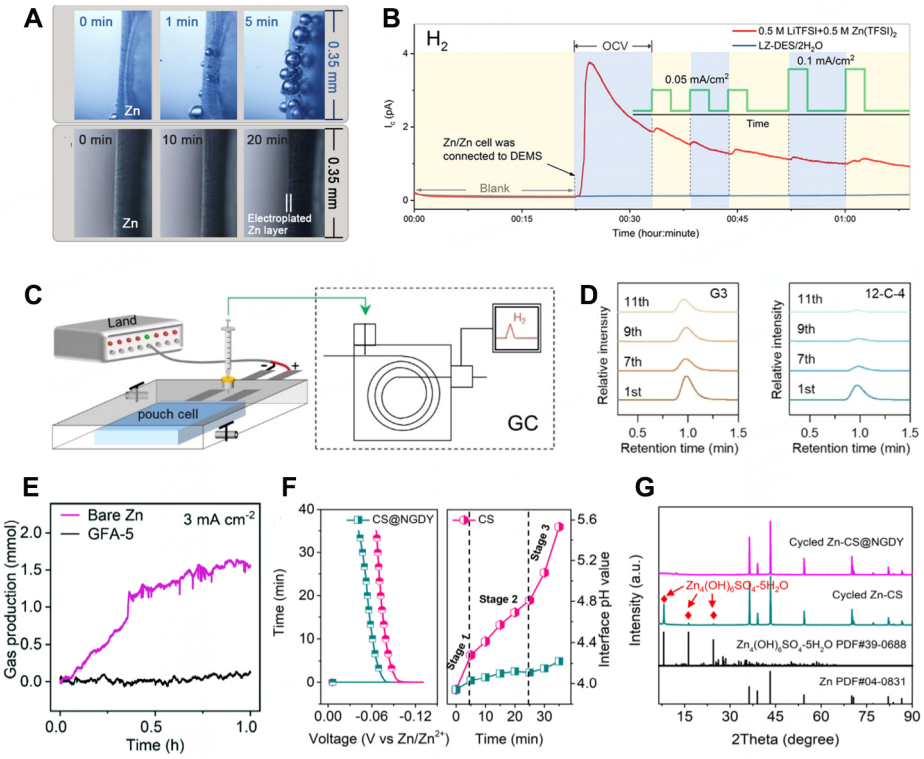

Figure 3. Hydrogen evolution in the aqueous ZIBs. (A) *In-situ* optical microscope observing the formation of bubbles at the anode surface. (B) Generation of H_2 gas under different charge-discharge states, demonstrated by DEMS[47]. Copyright 2019 Elsevier B.V. (C) Illustration of *in-situ* GC measurement by connecting the pouch cell and the GC equipment. (D) H_2 generation detected by GC at different cycles in different electrolytes[48]. Copyright 2023 John Wiley & Sons. (E) *In-situ* gas pressure detection for the batteries, with the evolution of gas generation converted to the amount of H_2 using the ideal gas equation[49]. Copyright 2022 The Royal Society of Chemistry. (F) Evolution of pH at different charge-discharge states. (G) X-ray diffraction (XRD) measurements demonstrating the generation of surface passivation of Zn anode in $ZnSO_4$ electrolyte after cycling[50]. Copyright 2022 John Wiley & Sons.

calendar aging. In contrast, the current collector shows the presence of dead Zn and void formation due to Zn corrosion.

Besides, the potential difference between the Zn and Cu collectors can further result in galvanic corrosion[53]. The Cu side acts as the electron acceptor, receiving electrons from the Zn anode and causing the generation of H_2 within the electrolyte, even when the system is operating under OCP. As shown in Figure 4G, upon immersing the anode into the electrolyte of 2 M $ZnSO_4$, a significant number of bubbles rapidly form. Furthermore, the size of these bubbles increases over time during immersion. Figure 4H illustrates the mechanism behind the capacity loss observed in ZIBs following calendar aging[52]. In contrast to LIBs, where continuous SEI forms on the anode surface in organic electrolytes, ZIBs with aqueous electrolytes experience anode corrosion and the formation of dead zinc, leading to a relatively shorter calendar life.

Another crucial aspect concerning the durability of ZIBs is the occurrence of overcharge conditions, which has been extensively studied in LIBs but has received relatively less attention in the case of ZIBs[54-60]. Aqueous batteries are regarded as having the ability to tolerate overcharging through the utilization of the "oxygen cycle", in which the gas generated during the overcharging process is reduced and reintroduced into the electrolyte [Figure 5A][5]. However, in the case of ZIBs, the oxygen cycle is not sustainable due to the lack of pH-buffering capability in the electrolytes. As a consequence, overcharging not only diminishes

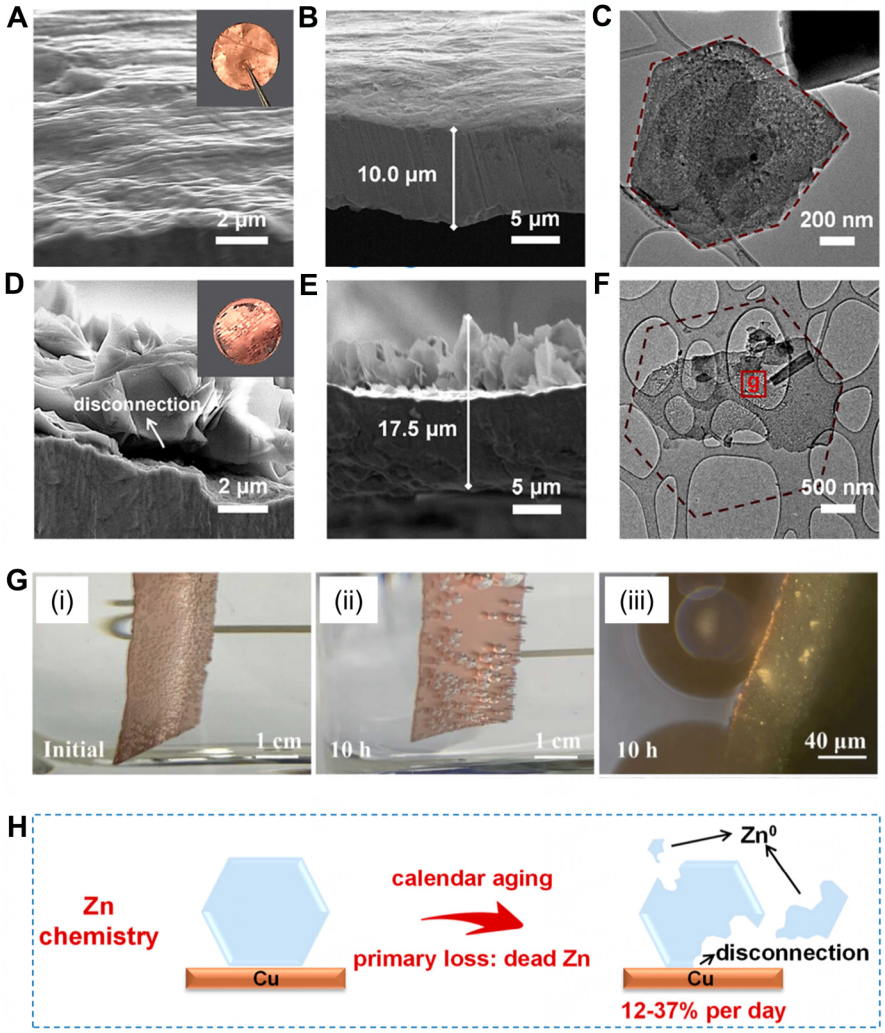

Figure 4. Calendar issues influencing the durability of ZIBs. SEM images of (A) the Cu surface and (B) the Cu thickness without aging. (C) TEM image of deposited Zn without aging. SEM images of (D) Cu surface and (E) Cu thickness after aging for 24 h. (F) TEM image of deposited Zn after aging for 24 h. Insets in (A and D) are the corresponding optical images[52]. Copyright 2023 American Chemical Society. (G) Optical images of hydrogen evolution in (i) the initial state; (ii) 10 h after electrode aging in the electrolyte; and (iii) Hydrogen bubble observed in an *in-situ* optical microscope[53]. Copyright 2021 John Wiley & Sons. (H) Illustration of the mechanism for the capacity loss in aqueous ZIBs during calendar aging[52]. Copyright 2023 American Chemical Society.

the overall capacity of the battery but also poses safety risks. The generated H_2 and O_2 can cause the battery to swell, potentially resulting in leakage or even explosion [Figure 5B][61].

To date, the investigation of overcharge behavior in batteries has been limited to batteries that employ an iodine (I_2) cathode[62]. As illustrated in Figure 5C-E, several significant observations can be made when the Zn||I_2 batteries are charged to potentials exceeding 1.6 V. Firstly, the CE of the batteries decreases, indicating a reduced reversibility in the charge-discharge process. Additionally, the pH value of the batteries increases, suggesting a shift towards a more alkaline environment. Finally, the capacity of the batteries undergoes degradation, indicating a gradual decline in stability. The decrease in stability is attributed not only to the irreversible conversion of I_2 to $Zn(IO_3)_2$ but also to the anode passivation associated with the transformation of Zn to ZnO at the anode [Figure 5F]. Thus, achieving a stable Zn anode is crucial for enhancing battery durability; however, this aspect has received less attention in research. Overcharging in

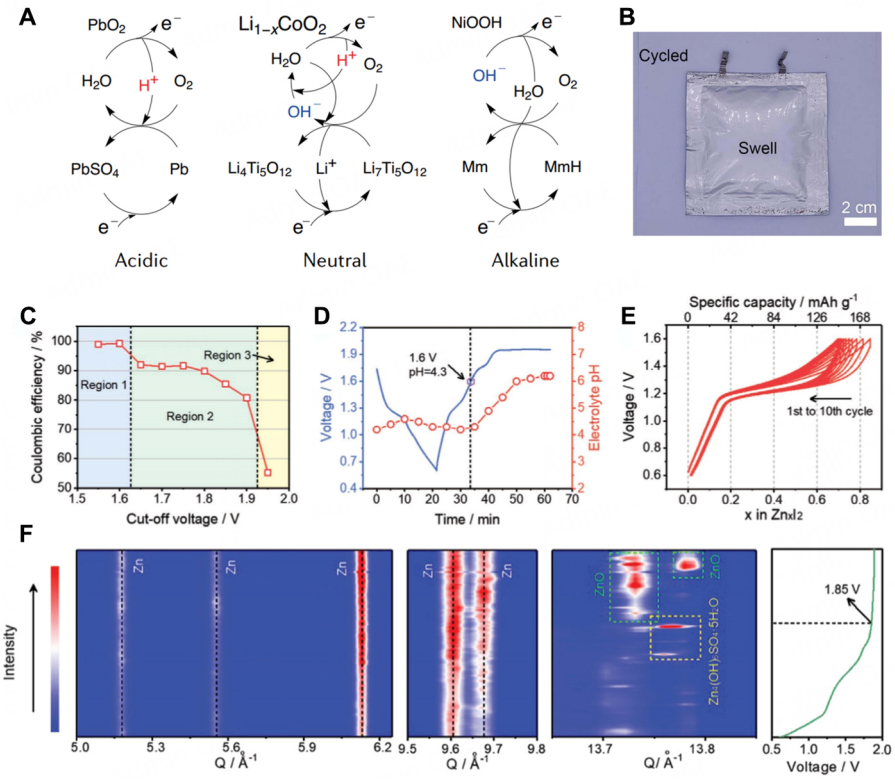

Figure 5. Overcharge-related issues impacting the durability of ZIBs. (A) Schematic illustration of the oxygen cycle in sealed aqueous batteries[5]. Copyright 2022 Springer Nature. (B) Optical images of battery swelling. Reproduced with permission under Creative Commons CC BY license from Ref.[61]. Copyright 2023 Springer Nature. Evolution of the (C) CE, (D) pH, and (E) specific capacity of Zn||I_2 battery under different operating voltages[62]. (F) Operando synchrotron XRD analysis of the Zn anode during the charging of ZIBs. Reproduced with permission from Ref.[62]. Copyright 2020 John Wiley & Sons.

ZIBs can result in several detrimental effects on the zinc anode. One major issue is accelerated dendrite formation, where excessive charging encourages rapid and uneven zinc deposition, leading to dendrites that can pierce the separator and cause short-circuiting. Additionally, overcharging increases the potential for hydrogen evolution, as water splitting at the anode surface generates hydrogen gas, depleting the electrolyte and creating internal pressure that poses safety risks. The decomposition of electrolyte components at high voltages can also produce by-products that adhere to the anode surface, forming an unstable, resistive interface. Furthermore, overcharging can exacerbate corrosion and surface degradation, especially when side reactions create localized acidic conditions that corrode the zinc, compromising the anode's structural integrity and reducing battery lifespan.

ADDITIVES REGULATING THE SOLVATION STRUCTURE

Reducing water activity

The solvation structure of Zn^{2+} plays a crucial role in the deposition behavior and reversibility of aqueous ZIBs, as it directly influences the reactions occurring on the zinc anodes. In aqueous electrolytes, Zn^{2+} ions exhibit a strong affinity for H_2O molecules. Consequently, each Zn^{2+} ion coordinates with five or six H_2O molecules, forming the $[Zn(H_2O)_5]^{2+}/[Zn(H_2O)_6]^{2+}$ complex, which constitutes the first solvation shell of Zn^{2+} [Figure 6A][63]. Recent research suggests that the evolution of H_2 gas in aqueous ZIBs predominantly arises from solvated H_2O molecules rather than water molecules not directly interacting with Zn^{2+} ions[64]. To prevent water-associated side reactions, replacing the H_2O molecules in the first solvation shell with other suitable molecules is crucial.

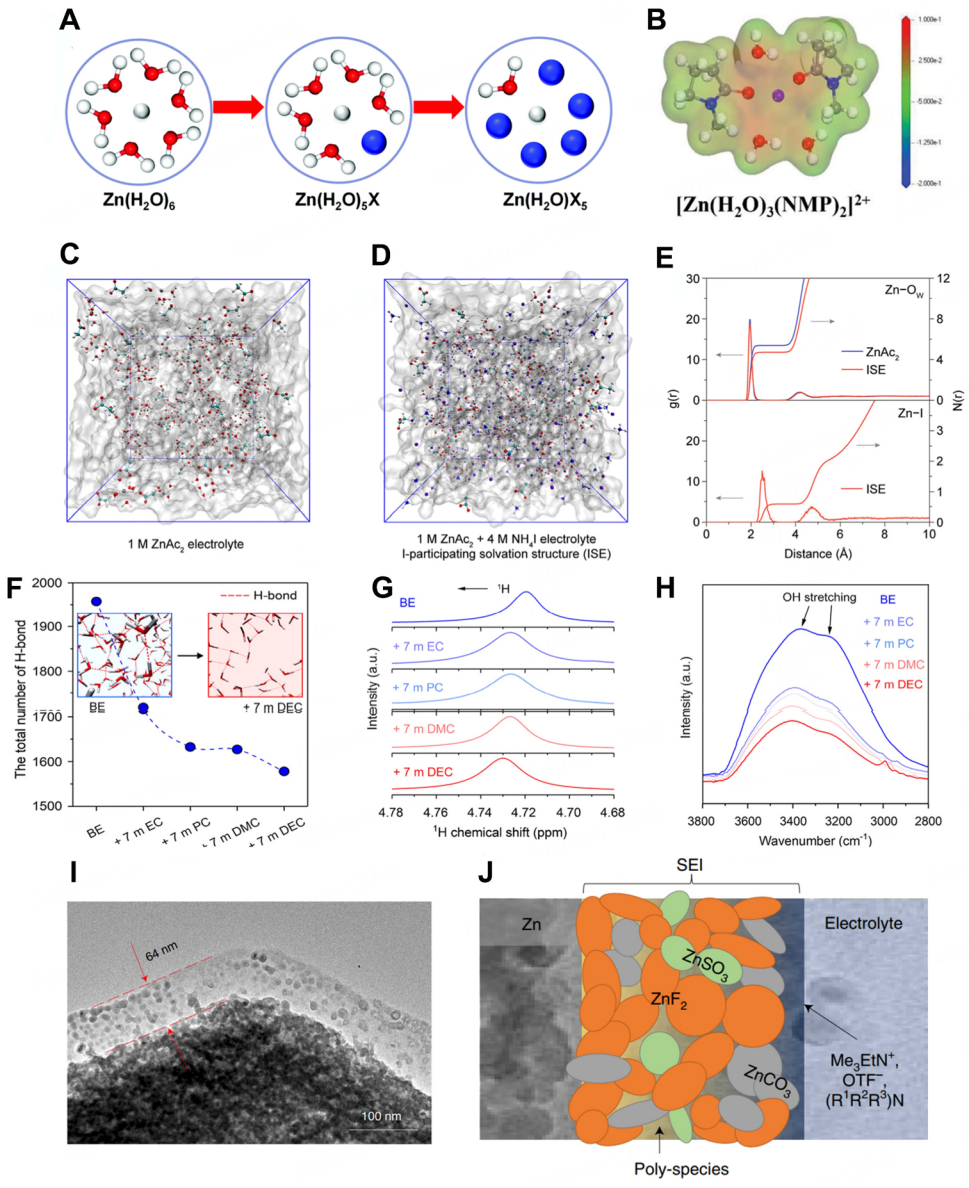

Figure 6. Electrolyte additive regulating the solvation structures of ZIBs. (A) Schematic illustration of the typical and the regulated Zn^{2+} solvation structures[63]. Copyright 2021 John Wiley & Sons. (B) ESP of Zn^{2+} solvation structure regulated by NMP with high donor number[66]. Copyright 2022 John Wiley & Sons. Molecular dynamics (MD) snapshots of (C) 1 M $Zn(Ac)_2$ and (D) 1 M $Zn(Ac)_2$ + 4 M NH_4I electrolyte, along with the corresponding (E) RDF and CN curves[67]. Copyright 2022 American Chemical Society. (F) Total number of hydrogen bonds in the electrolytes with different concentrations of additives. (G) NMR and (H) FTIR spectra demonstrate the breaking of hydrogen bonds in the electrolytes[70]. Copyright 2022 American Chemical Society. (I) TEM images and (J) illustration of the composition of the SEI layer on the anode surface with electrolyte additives[71]. Copyright 2021 Springer Nature.

Organic molecules with a higher Gutmann donor number than H_2O are commonly used as additives in ZIBs[65]. These additives preferentially form solvated ions with Zn^{2+}, repelling the H_2O molecules in the first solvation shell. Figure 6B shows the electrostatic potential (ESP) mapping of the *N*-methyl-2-pyrrolidone (NMP)-modified Zn^{2+} solvation structures[66]. It can be inferred that the two H_2O molecules in the solvation shell are replaced by the NMP molecules, forming a new complex: $[Zn(H_2O)_3(NMP)_2]^{2+}$. The reorganization of the solvation shell not only leads to a reduction in solvated H_2O molecules but also alleviates the

repulsion force, thereby restraining the side reactions and facilitating the accelerated migration of ions. To date, numerous organic additives, such as glucose, dimethyl sulfoxide (DMSO), methanol (MeOH), glycerol, ethylene glycol (EG), triethyl phosphate (TEP), diethyl carbonate (DEC), hexamethylphosphoric triamide (HMPA), and propylene carbonate (PC), have been successfully employed to regulate the solvation structures and enable stable zinc anodes[29]. These organic additives consist of functional groups, such as C=O, P=O, or S=O, that have a strong affinity for zinc ions and play a crucial role in regulating the solvation structures.

Another additive that can tune the solvation structure of Zn^{2+} is inorganic or organic salts containing halogenated anions such as I^- or Cl^-. As an example, the introduction of NH_4I into the electrolyte containing 1 M zinc acetate [$Zn(Ac)_2$] can regulate the $[Zn(H_2O)_6]^{2+}$ solvation structure into a $[ZnI(H_2O)_5]^+$ solvation structure, which leads to a decrease in the CN of Zn^{2+} and H_2O pairs, as well as the observation of additional Zn-I coordination [Figure 6C-E][67]. Similar regulation of the solvation structure by halogenated anions has also been observed with other electrolyte additives, such as $ZnCl_2$ and 1-ethyl-3-methylimidazolium chloride (EMIMCl)[68,69]. All these electrolyte additives aim to disrupt the strong coordination between Zn^{2+} and H_2O, thereby inhibiting hydrogen evolution and other water-related side reactions.

In addition to reducing the amount of bound water in the solvation shell, introducing additives to regulate the solvation structure can also disrupt the hydrogen bond networks of water[70]. As illustrated in Figure 6F, MD simulations demonstrate a decrease in the total number of hydrogen bonds in the electrolytes upon the addition of DMC. The disruption of the hydrogen bond networks of water is further confirmed by NMR [Figure 6G] and FTIR spectra [Figure 6H], indicating a reduction in water reactivity and an increase in the stability of Zn anodes.

SEI formation

Traditionally, it was believed that the formation of a SEI layer in aqueous electrolytes did not occur until recent research demonstrated the effectiveness of incorporating additive DMSO[65]. Since then, numerous additive designs have been developed to promote the formation of an SEI layer on the Zn anode, providing protection against direct contact with water while allowing the transport of Zn^{2+}[71,72]. A common feature of the surface of a dense SEI layer on a Zn anode can be observed using TEM, which is several nanometers thick and composed of organic compounds that contribute to mechanical properties and inorganic compounds that facilitate ion conduction [Figure 6I and J][71,73].

Numerous organic additives have been reported to possess the ability to promote the *in-situ* formation of the SEI through their decomposition[74]. Additionally, the solvation environment of Zn^{2+} ions regulated by additives typically includes anions such as $TFSI^-$ and OTF^-[75]. During the electrodeposition process, these anions undergo decomposition and actively contribute to forming an SEI layer enriched with fluoride. Another type of additive playing a role in the formation of the SEI is water-reactive additives, including organic compounds such as fluoroethylene carbonate (FEC) and inorganic compounds such as KPF_6[76,77]. These additives can react with water, leading to the generation of active compounds such as HF and phosphoric acid. Following this, the compounds react with Zn to produce an inorganic SEI layer, such as $Zn_3(PO_4)_2$ and ZnF_2.

Regulating ion transport

The introduction of most electrolyte additives, which effectively regulate the solvation structures, usually results in a reduction in the ionic conductivity of commonly used electrolytes containing $ZnSO_4$, $Zn(OTF)_2$, or $Zn(TFSI)_2$[78]. The decrease in ionic conductivity can be attributed to the increase in the size of the solvation shell surrounding the Zn^{2+} ions, which in turn hinders the migration of the solvated Zn^{2+} ions. In

general, an increased concentration of additives in the electrolyte solution can result in higher viscosity, leading to lower ionic conductivity [Figure 7A][79]. Therefore, selecting an appropriate electrolyte additive concentration is crucial to effectively stabilize the Zn anode while maintaining a high ion transportation rate. Several additives, such as LiCl and sodium tartrate, have been reported to exhibit higher overall ionic conductivity than the blank electrolytes[80,81]. However, it should be noted that the diffusion of Zn^{2+} ions was not specifically addressed in these studies.

Even though the electrolyte additives modifying the solvation structures may have a negative impact on the ionic conductivities, the transference number of Zn^{2+} can be significantly increased by immobilizing the anions within the electrolyte[80]. As shown in Figure 7B, incorporating β-cyclodextrin (β-CD) additives with a hydrophobic inner cavity into the $Zn(ClO_4)_2$ system enables interaction with the ClO_4^- ions, as evidenced by the observed adsorption energy of -2.97 eV. Furthermore, the independent gradient model (IGM) analysis indicates that the affinity between β-CD and the ClO_4^- is primarily due to H bonding, with a minor contribution from van der Waals forces [Figure 7C]. Consequently, including the additive effectively impedes the association between the anion and cations, thereby enhancing the diffusion coefficient of Zn^{2+} and resulting in a significant increase in the transfer number from 0.457 to 0.878.

In addition to β-CD, several other additives have been reported to enhance the transference number in electrolytes, such as xylitol[81], D-arabinose[82], cucurbituril[83], and tris[84]. More recently, tetraphenylporphyrin tetrasulfonic acid (TPPS), with the ability to form large molecule aggregates within the electrolytes, has been reported to increase the Zn^{2+} transference number from 0.31 to 0.95 [Figure 7D-F][85]. The density functional theory (DFT) simulations uncover distinct interactions between TPPS and various anions, which can be attributed to the differences in size, charge, and symmetry. The charge densities of SO_4^{2-}, ClO_4^-, and BF_4^- are considerably higher compared to those of Cl^- and acetate (Ac^-), thus contributing to the higher interactions with TPPS and remarkably enhanced transference numbers [Figure 7G].

ADDITIVES REGULATING THE EDL

By regulating the EDL, additives promote a more even distribution of Zn^{2+} across the surface. This results in a smoother, more uniform deposition that reduces the formation of needle-like dendrites, which can otherwise lead to short circuits and degrade battery performance. In addition, the improved uniformity helps prevent localized over-deposition, minimizing the formation of inactive "dead zinc" deposits. Overall, additives not only lower the risk of dendrite formation but also enhance the cycling stability and efficiency of the anode, thereby improving the utilization rate of the zinc metal.

SEI formation

As previously mentioned, including additive molecules in the solvation structure can result in the formation of the SEI layer through the decomposition or reaction with the aqueous solution. However, altering the solvation structure requires the additive to be present at a certain concentration, which can adversely affect the migration of Zn^{2+}. In contrast, employing additives in trace amounts to modulate the EDL instead of the solvation structure offers a promising solution[86].

Figure 8A illustrates the molecular structures of various electrolyte additives, namely methanol (M1), ethanol (M2), 2-propanol (M3), acetone (M4), dimethyl carbonate (M5), sulfolane (M6), N-methylpyrrolidone (M7), N,N-dimethylformamide (M8), glycerol (M9), 1,2-dimethoxyethane (M10), bis(2-methoxyethyl)ether (M11), 1,3-dioxolane (M12), ethylene carbonate (M13), propylene carbonate (M14), and ethylene glycol (M15)[87]. The characterization using Raman spectra and differential capacitance

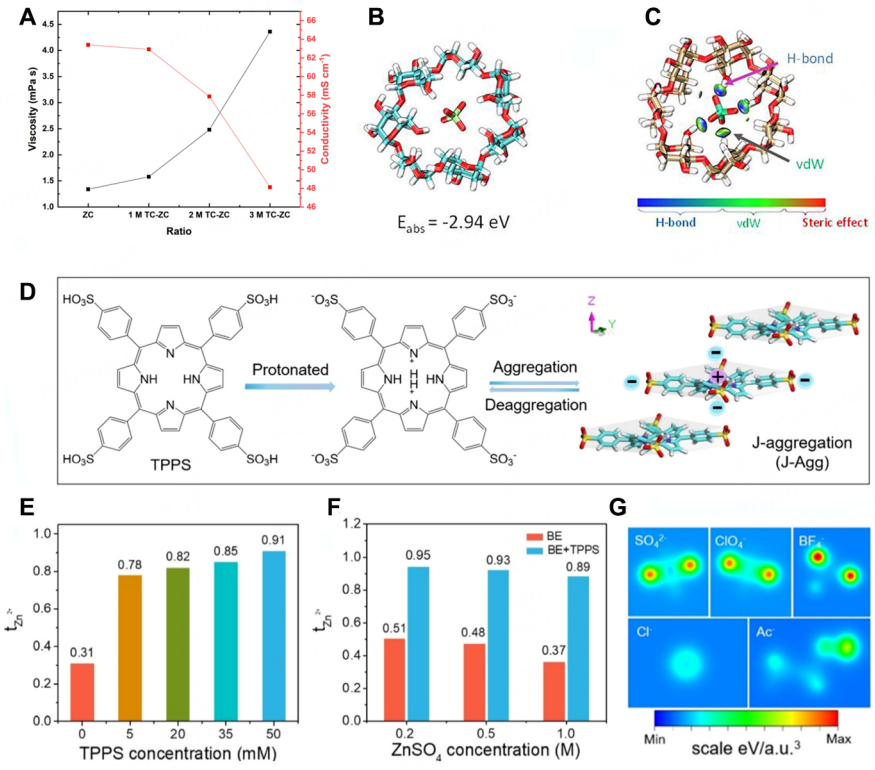

Figure 7. Electrolyte additives regulating the ion transport of ZIBs. (A) Relationship between the additive concentration and the velocity and conductivity of the electrolyte[79]. Copyright 2022 John Wiley & Sons. (B) DFT calculations reveal an adsorption energy of -2.97 eV between β-CD and ClO_4^-. (C) IGM analysis of the β-CD@ClO_4 complex showcasing blue for electrostatic interactions (such as hydrogen bonding), green for van der Waals interactions, and red for steric effects[80]. Copyright 2022 John Wiley & Sons. (D) Illustration depicting the formation process of TPPS aggregates in the electrolytes. Zn^{2+} transference numbers in electrolytes with varying concentrations of (E) TPPS and (F) $ZnSO_4$. (G) Charge densities of different anions. Reproduced with permission from Ref.[85]. Copyright 2024 John Wiley & Sons.

measurements suggests that these additives primarily influence the EDL structure while having little to no effect on the solvation structure [Figure 8B and C] with a minimal addition of 1 vol%. Consequently, only a select few additives exhibit effective stabilization of the Zn anode, while their impact becomes more pronounced with higher concentrations. Among these additives, M6 (sulfolane) and M11 [bis(2-methoxyethyl)ether] have demonstrated the most promising performance. Further investigation through DFT calculations reveals that factors influencing the structure, such as the lowest unoccupied molecular orbital (LUMO), dipole moment, donor number, and adsorption energy, do not significantly affect the system under minimal additive concentrations[88]. On the contrary, the additive's capacity to establish a SEI layer is of paramount importance in ensuring the stability of the zinc anode [Figure 8D].

Furthermore, the variation in additive anions also contributes to forming a distinct SEI layer in addition to the organic molecules[26]. As shown in Figure 8E, Ac^- and trifluoroacetate (TFA^-) anions, which possess contrasting polarities, were incorporated into the baseline electrolyte of 2M $Zn(OTF)_2$. The elevated adsorption energy of Ac^- anions due to their stronger polarity contributes to forming a more compact Helmholtz layer, in contrast to the TFA^- anions. This preference for Ac^- anions facilitates the formation of a uniform and dense SEI layer, which in turn enhances the suppression of water-induced side reactions [Figure 8F-H].

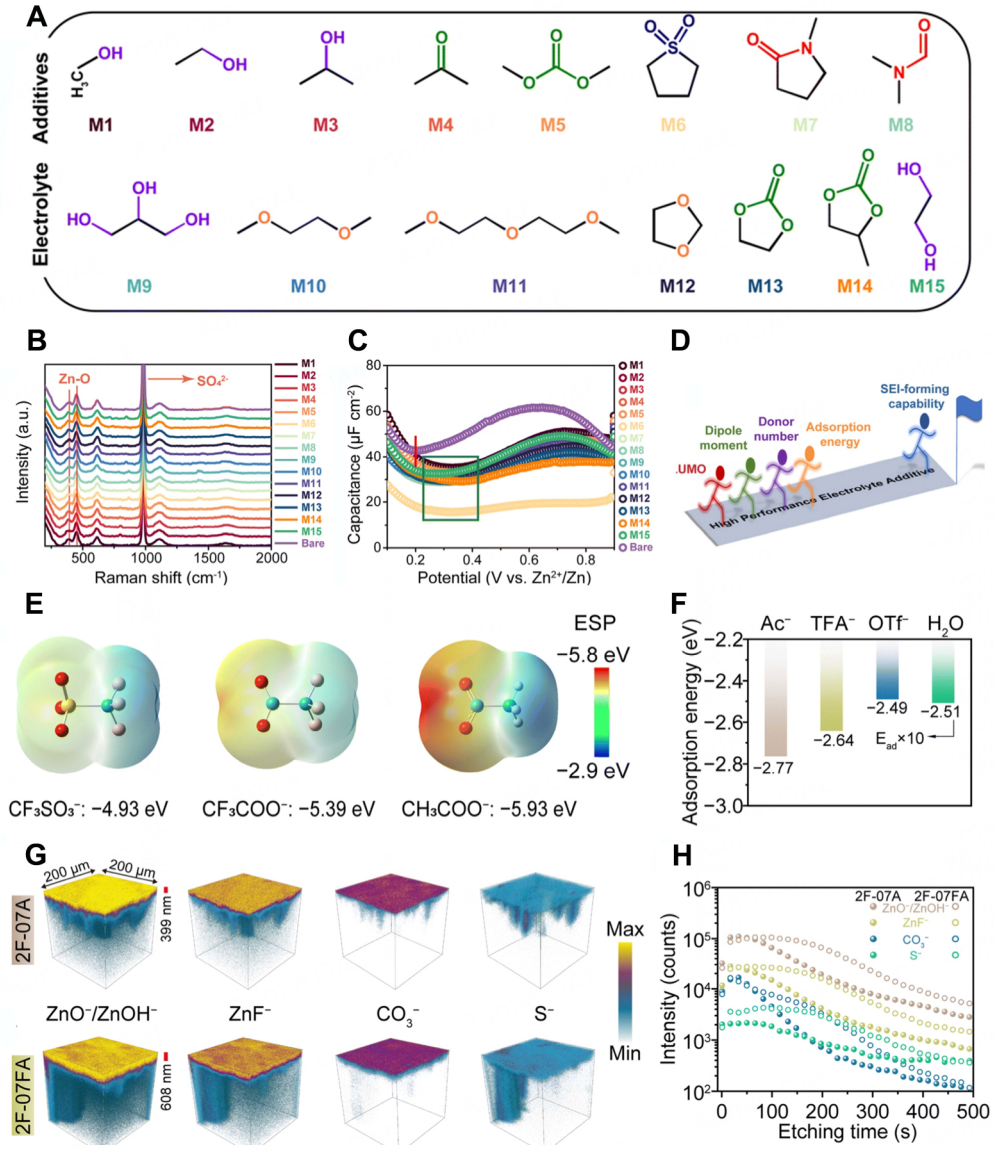

Figure 8. (A) Illustration of the molecular structures of various electrolyte additives. (B) Raman spectra and (C) differential capacitance measurements suggesting the modification of additives on the EDL rather than the solvation structure with a minimal addition of 1 vol%. (D) Illustration of the factors that may impact the electrodeposition morphology[87]. Copyright 2023 The Royal Society of Chemistry. (E) ESP mapping of different anions, showing the varying polarity of OTF^-, TFA^-, and Ac^-. (F) Adsorption energy of different anions and water molecules on the Zn(101) plane. (G) Three-dimensional (3D) reconstruction maps of Zn electrodes obtained from different electrolytes, as measured by ToF-SIMS. (H) Corresponding ToF-SIMS depth profiles of major secondary ions with 2F-07A and 2F-07FA electrolytes[26]. Copyright 2024 The Royal Society of Chemistry.

SEI formation through the regulation of solvation often requires additives in high concentrations, which can negatively impact properties such as ionic conductivity, thereby affecting overall performance. On the other hand, SEI formation through EDL regulation typically needs additives in lower concentrations, resulting in minimal impact on overall performance. However, most current reports are focused on the former, while research based on the latter is relatively scarce.

Surface adsorption

Some electrolyte additives have the ability to regulate the deposition of zinc without forming an SEI layer but rather through adsorption on the surface of the anode. One typical mechanism for this phenomenon is the modification of the electrocrystallization morphology[89]. As shown in Figure 9A, the electrocrystallization morphology is related to the mass transfer, charge transfer, and adatom self-diffusion. Theoretically, the Zn (0001) face, characterized by the lowest surface energy, should be conducive to dendrite-free growth[90]. However, due to the roughness of the anode surface, which results in non-uniform electric field distribution (known as the tip effect), the growth of crystalline zinc does not occur under equilibrium conditions. Dendrite formation occurs on the surface of the anode due to the slower mass transport in the electrolyte compared to the electrochemical reduction rate [Figure 9B]. Considering these factors, achieving a layer-like deposition of zinc can be facilitated by shifting the control from diffusion to activation by introducing suitable additives at the EDL [Figure 9C].

The cyclic tetramethylene sulfone (TMS), with its ESP mapping revealing distinct electrophilic and nucleophilic sites, tends to adsorb vertically on the Zn anode [Figure 9C and D]. Furthermore, the presence of TMS molecules in the IHP significantly diminishes the interaction between the anode and solvated ions, resulting in a reduction in the electrochemical reduction process [Figure 9E]. This shift towards activation control ultimately influences the deposition process. Based on the X-ray diffraction (XRD) results, adding TMS facilitates forming a preferred orientation along the (0001) plane [Figure 9F]. The (0001) pole figures of the Zn anodes using different electrolytes provide further evidence that the decreased electrochemical reaction rate promotes the formation of (0001) texture, resulting in compact and planar growth of the Zn crystals [Figure 9G and H].

Furthermore, electrolyte additives with a high donor number can effectively eliminate H_2O molecules from IHP, in addition to regulating electrocrystallization[27]. This process reduces the solvated H_2O density and promotes the homogeneous deposition of Zn [Figure 9I]. Pyridine (Py), with its higher donor number than dimethylformamide (DMF) and MeOH [Figure 9J], exhibits a stronger coordination capability towards Zn^{2+}. The distinctive architecture of the IHP prevents the inclusion of solvated H_2O molecules within the solvation shell of Zn^{2+}, even with introducing a small proportion of Py into the electrolytes. Consequently, adding the electrolyte additive enables effective suppression of H_2O activity without compromising ion migration within the bulk electrolyte.

Electrostatic shielding

The concept of employing an electrostatic shielding stabilized anode, in which Cs^+ and Rb^+ were used as electrolyte additives, was the earliest reported in LIBs[91]. In order to achieve planar Zn morphology, several inorganic additives, such as Y^{3+}[92], Li^+[93], Na^+[94], Ce^{3+}[95], Mg^{2+}[96], and Mn^{2+}[97], have been employed based on the mechanism of electrostatic shielding. Furthermore, organic cations, such as 1-ethyl-1-methyl pyrrolidinium (EMP^+)[98], 1-ethyl-3-methylimidazolium ($EMIM^+$)[68], and positively charged chlorinated graphene quantum dots (Cl-GQDs)[99], have also been reported to exhibit electrostatic shielding properties.

The mechanism of electrostatic shielding is illustrated in Figure 10A and B. In the absence of electrolyte additives, the growth of zinc atoms would occur randomly, leading to the formation of dead zinc and dendrites[92]. After introducing cations into the electrolyte with lower reduction potentials than Zn^{2+}/Zn, they would preferentially accumulate around the tips of the zinc electrode due to the higher electric field strength. This process prevents Zn^{2+} ions from depositing near the tip regions and protects the Zn anode from direct contact with water, thus helping to restrict side reactions and dendrite formation.

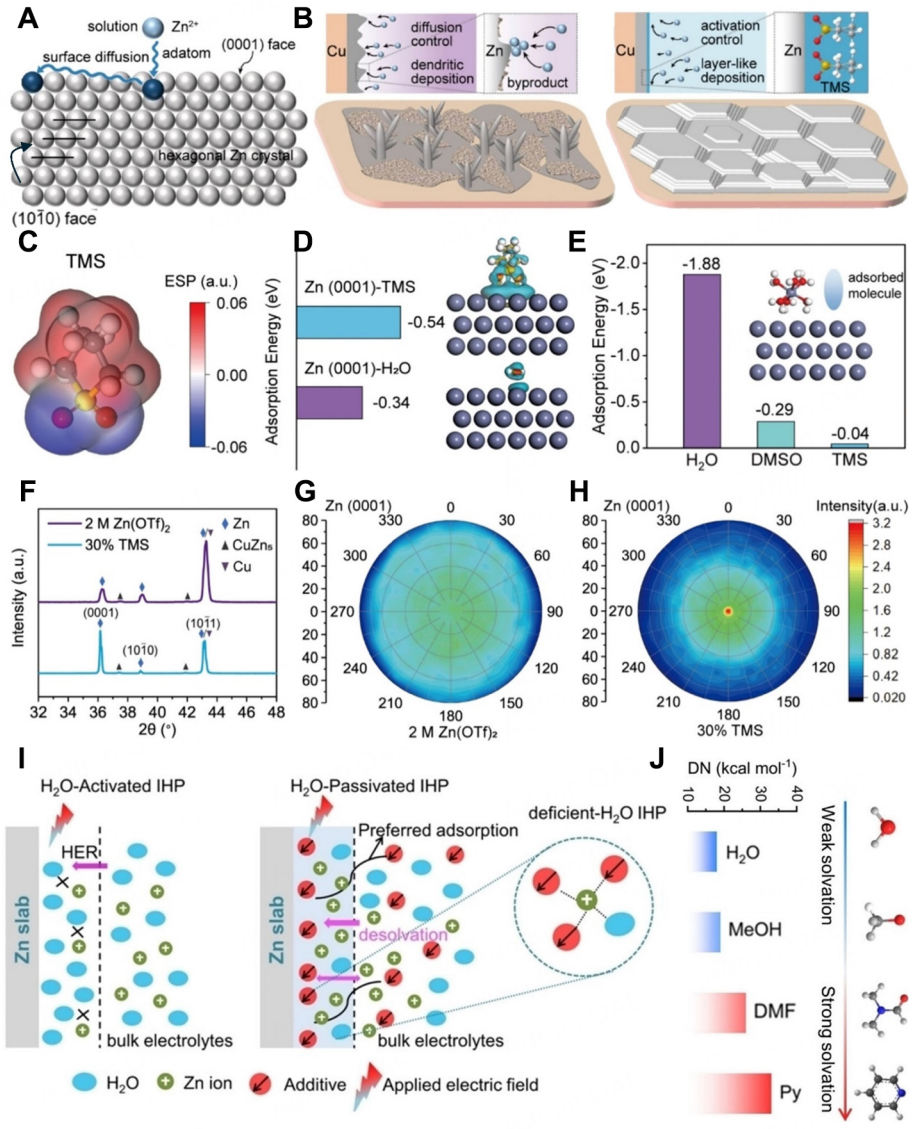

Figure 9. (A) Schematic representation of the growth of hexagonal Zn crystals. (B) Proposed mechanism of Zn electrodeposition under diffusion control and activation control. (C) ESP mapping of TMS. (D) Diagrams showing the difference in charge density of H_2O and TMS molecules on the Zn (0001) plane, along with their corresponding adsorption energy values. (E) Adsorption energy values of solvated Zn^{2+} on the Zn (0001) plane with adsorbed molecules. (F) XRD patterns of deposited Zn in different electrolytes. Pole figures of the Zn anodes prepared in the electrolyte (G) without and (H) with electrolyte additive[90]. Copyright 2023 John Wiley and Sons. (I) Schematic representation of the IHP regulated by additive with high donor number. (J) Summary of the coordination power of the different additives[27]. Copyright 2023 John Wiley and Sons.

Using locally magnified *in-situ* microscopy images provides visual evidence of the distinct deposition behaviors observed with different electrolytes. As depicted in Figure 10C, zinc atoms tend to aggregate at the tip region of the anode in the $ZnSO_4$ electrolyte, leading to rapid growth and an uneven surface under the influence of the electric field. In contrast, the Y^{3+} ions demonstrate dynamic and self-regulating behavior during deposition. Their occupation of the top site effectively excludes Zn ions, allowing the Zn ions to grow at the bottom positions. Furthermore, alongside experimental results, finite element modeling (FEM) simulations offer supplementary evidence to elucidate the mechanism of the electrostatic shielding effect [Figure 10D-F][95]. The Zn anode initially exhibits a semi-elliptical shape, with a higher deposition of Zn

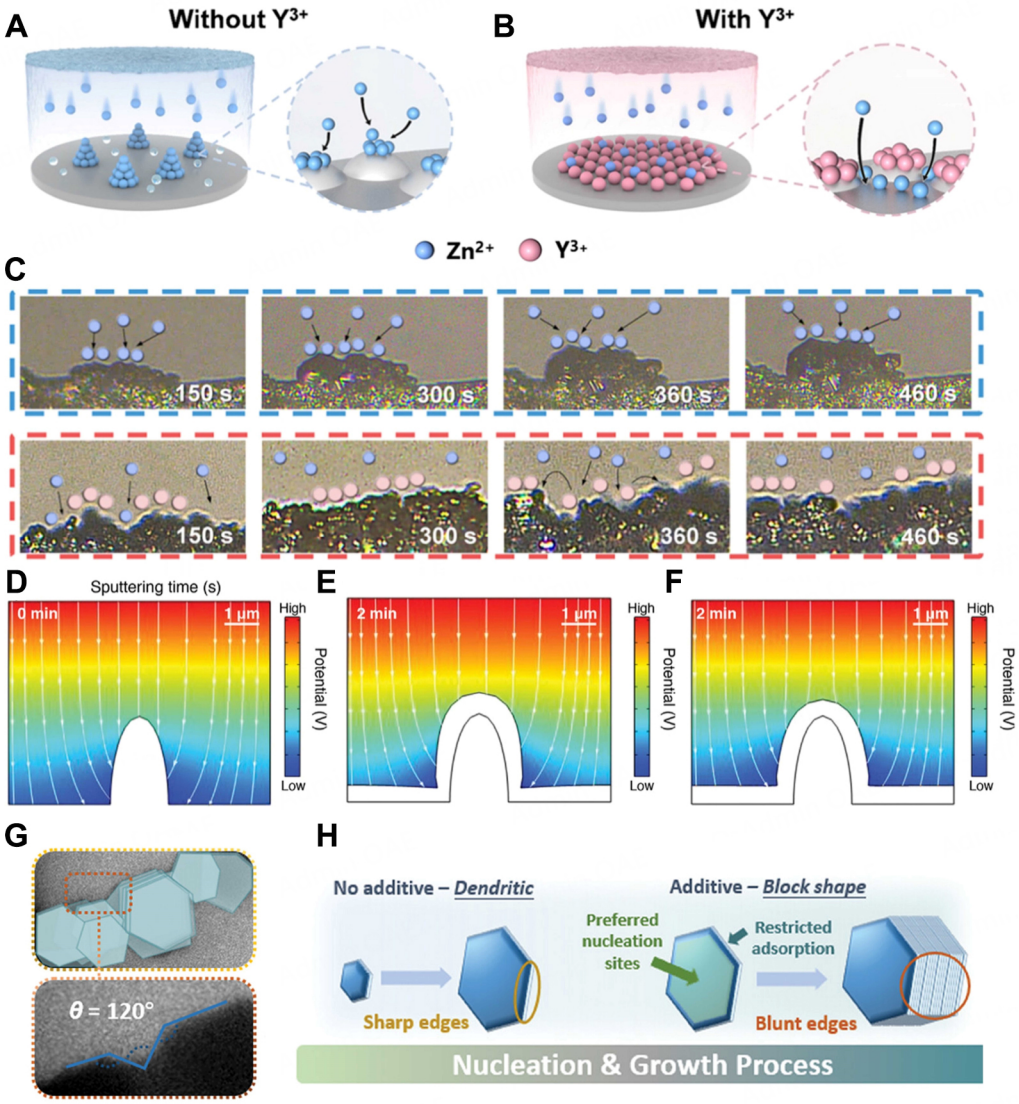

Figure 10. Schematic illustration of Zn deposition in the electrolytes without (A) and with (B) electrostatic shielding effect. (C) Locally magnified *in-situ* microscopy images showing the deposition behavior in the electrolyte without (top) and with (bottom) electrostatic shielding effect[92]. Copyright 2023 Elsevier B.V. FEM simulation of the Zn anode (D) at the initial state, (E) after deposition in the electrolyte without electrostatic shielding effect, (F) after deposition in the electrolyte with electrostatic shielding effect[95]. Copyright 2022 John Wiley and Sons. (G) Magnified and annotated images of Zn deposition morphology were acquired for *in-situ* electrochemical transmission electron microscopy (TEM) imaging (top), and magnified images showing Zn deposition with the inter-island mergence angle indicated (bottom). (H) Schematic illustration of the possible mechanism leading to the formation of Zn blocks with electrostatic shielding effect[100]. Copyright 2024 John Wiley and Sons.

around the cusps rather than the flatter regions of the anode in the $ZnSO_4$ electrolyte. Upon the introduction of cations into the electrolyte, the enriched cations at the top region exert a pronounced electrostatic shielding effect on Zn^{2+}, facilitating the deposition of Zn^{2+} on the smoother regions of the anodes.

More recently, a novel Electrostatic Shielding Mechanism has been proposed according to the observation of operando electrochemical TEM [Figure 10G and H][100]. Contrary to the previously proposed theory of preferential adsorption at sharp edges, the authors highlight that the electrostatic shielding effect prevents

secondary Zn nucleation on Zn (100) faces. Instead, it promotes deposition on Zn (002) faces, resulting in blockier morphologies and ultimately leading to a denser and smoother anode surface after charging. The electrodeposition of metals involves a series of sequential steps, including diffusion, adsorption, desolvation, electron transfer, and self-diffusion [Figure 1F][29]. Initially, the solvated metal ions from the bulk electrolyte would migrate towards the electrode substrate through diffusion and subsequently be absorbed on the OHP. Following this, the solvated ions undergo a gradual desolvation process, transforming into desolvated ions, which then transport to the IHP. Once the desolvated metal ions reach the IHP, the desolvated metal ions may gain electrons from the electrode, reducing the desolvated metal ions and the subsequent formation of metal atoms. Finally, metal atoms migrate along the substrate surface, forming strong chemical bonds at active sites, and then enter the crystal lattice[31].

Another extensively studied theory in electrodeposition is the Marcus-Hush model, which proposes that the reduction of metal ions occurs through an outer-sphere electron transfer reaction within the EDL structure[32]. According to this theory, the electron transfer initially occurs to the solvated cations in the outer sphere, reducing these cations into metal atoms that subsequently adsorb onto the metal surface. In this process, the solvated ions do not need to cross the interface, although their distance from the metal surface may vary slightly[33-36].

However, recent studies have revealed that the removal of the solvation shell and the reduction of effective charge on metal ions occur through numerous small steps involving a mechanism of formation followed by rupture[37]. When both mass and charge cross the interface, the charge must be carried by the ion species rather than electrons due to the significant difference in timescales for electron and ion transfer[33]. As the electrons transfer to the solvated cations, the solvation structure of the cations concurrently undergoes reorganization to lower the system's energy [Figure 1G][30,38]. The solvated cations with lower valency ultimately traverse the double layer and are reduced to metal atoms.

As mentioned above, hydrogen evolution can be inhibited by adjusting the solvation structure or regulating EDL. Combined with gas chromatography experiments and calculations, Yang *et al.* demonstrate that by reducing solvated water with glycine additives, hydrogen evolution and "parasitic" side reactions on the Zn anode are inhibited[64]. Li *et al.* use a small amount of sodium 4-aminobenzenesulfonate (SABS) to induce uniform Zn^{2+} deposition and suppress side reactions[101]. The adsorption of SABS facilitates the formation of an IHP lacking H_2O molecules, which inhibited hydrogen evolution and corrosion from free H_2O molecules on the Zn anode[101].

It is worth mentioning that additives play a crucial role in improving the performance of solid-state ZIBs, including hydrogel-based systems. The current solid-state zinc batteries typically still contain small amounts of water or organic solvents. Ion transport is particularly important given the challenges of ion movement in solid-state and hydrogel electrolytes compared to liquid systems. Similar to the aforementioned functions in an aqueous system, additives can also regulate the solvation structure and the EDL of quasi-solid ZIBs. The introduction of certain additives can also help mitigate cathode dissolution, such as $Mn(CF_3SO_3)_2$[102], $MnSO_4$, and $CoSO_4$[103]. In hydrogel-based solid electrolytes, additives also contribute to increased mechanical stability and flexibility, making them ideal for wearable or flexible battery applications where resilience is essential[104]. Finally, we summarize and compare the performance of aqueous ZIBs with additives, particularly at low N/P ratios [Table 1]. Currently, achieving long cycle life remains a challenge under low N/P ratios.

Table 1. A summary of recently reported electrolyte additives and representative electrochemical performances in ZIBs with a low N/P ratio

Additive name	Electrolyte	Effects	Performances (capacity/lifespan/retention)	N/P ratio	Ref.
N-methyl pyrrolidone (NMP)	5% NMP + 2 M $ZnSO_4$	Regulate solvation structures	MnO_2||Zn 5.05 mAh cm^{-2} 100 cycles (82.6%)	2.3	[105]
SeO_2	2 mM SeO_2 + 2 M $ZnSO_4$	Induce the formation of SEI	MnO_2||Zn 1.21 mAh cm^{-2} 60 cycles (105.6%)	4.2	[106]
2-hydroxy-4′-(2-hydroxyethyl)-2 Methylpropiophenone (irgacure2959)	2 M $ZnSO_4$ + 0.44 mM/0.1 g L^{-1} irgacure2959	Induce anode morphology	VS_2||Zn 151 mAh g^{-1} 500 cycles (89.1%)	2.5	[107]
Propylene glycol	2 M $ZnSO_4$-50 vol% propylene glycol	Induce anode morphology	MnO_2||Zn 114.7 mAh g^{-1} 300 cycles (84.6%)	8.3	[108]
Sodium tartrate	1 M $ZnSO_4$ + 0.01 M sodium tartrate	Induce anode morphology	MnO_2||Zn 122.4 mAh g^{-1} 1,000 cycles (37.9%)	10	[109]
Azithromycin	2 M $ZnSO_4$ + 0.1 M azithromycin	Regulate solvation structures	V_2O_5||Zn 338.1 mAh g^{-1} 500 cycles (83.5%)	3.6	[110]
Dimethylacetamide/trimethyl phosphate (DMAC/TMP)	1 M $Zn(OTf)_2$ in (5:3:1 volume ratio) DMAC/TMP/H_2O	Regulate solvation structures	NaV_3O_8·1.5H_2O||Zn 187.3 mAh g^{-1} 3,000 cycles (65.1%)	5	[111]
1,2-dimethoxyethane (DME)	1 M $Zn(OTf)_2$ in DME + H_2O (0.15:1 molar ratio)	Regulate solvation structures	V_2O_5||Zn 186.2 mAh g^{-1} 50 cycles (91%)	3.56	[112]

CONCLUSION

In summary, this review has provided a comprehensive analysis of the up-to-date strategies for enhancing the stability and extending the lifespan of Zn anodes in aqueous ZIBs by strategically introducing appropriate additives into the electrolyte. Through detailed discussions on the roles of various additives, this review has highlighted how the electrolyte additives influence the solvation and the EDL structure of the electrolytes, thereby mitigating detrimental dendrite formation and side reactions. Significant achievements have been realized in the development of zinc anodes, with lifespans extending to several thousand hours and cumulative plated capacities surpassing 5,000 mAh cm^{-2}. Despite the significant progress achieved, several issues still exist and require further exploration.

Firstly, most research concerning electrolyte additives for Zn anodes is conducted using coin cells. This approach may not accurately represent the performance of zinc anodes in larger or more practical battery systems. Some investigations have reported the preparation of pouch-type full cells; however, most of these studies are based on thick zinc configurations with limited zinc utilization. Additionally, the reported pouch cells typically deliver relatively low overall capacities of around 100 mAh and low areal capacities, which fall short of the practical requirements for batteries in terms of energy density. Furthermore, the degradation mechanisms of zinc anodes in pouch cells, particularly when employing ultrathin zinc metal anodes, may exhibit considerable differences at an expanded scale, necessitating comprehensive analysis.

Secondly, issues related to enhancing the energy density of ZIBs require careful consideration for Zn anodes. The energy density of ZIBs is influenced not only by the mass of cathode and anode materials but also by other essential components contributing to overall energy densities. For instance, the performance evaluation of Zn anodes typically involves thick glass fiber separators with a thickness of approximately 1.0 mm, which significantly exceeds the thickness of separators used in commercial LIBs, typically less than 40 μm. Therefore, factors such as depth of discharge, the capacity ratio between anodes and cathodes, electrolyte volume, and the properties of separators must be meticulously evaluated during the development of the appropriate electrolyte additive for a stable Zn anode.

Lastly, although substantial focus has been placed on the stability of batteries, specifically the cycling stability, research concerning the durability of these systems has been relatively lacking. Durability is essential for practical applications, as the ability to maintain the reliability of ZIBs under calendar aging conditions, mechanical vibrations, overcharge scenarios, and fluctuations in temperature and humidity is crucial for the storage, transportation, and utilization of these batteries. Previous research indicates that the evolution of Zn anodes during operation is a significant factor in the degradation of battery durability. However, related studies have primarily focused on calendar aging conditions and overcharge scenarios. Therefore, investigations into the durability of Zn anodes under various conditions are highly valuable and notably overlooked. Furthermore, developing appropriate electrolyte additives to enhance the durability of Zn anodes is highly beneficial for the durability of ZIBs. However, current research in this area is lacking, making it a valuable and promising direction for further study.

Ideal properties for electrolytes in ZIBs include high ionic conductivity for effective Zn^{2+} transport, wide electrochemical stability window to withstand high operating voltages without degradation or gas evolution, and low reactivity with Zn anodes to minimize side reactions, thereby extending the cycle life of the battery and enhancing overall performance.

Strategies for electrolyte modification can include not only the introduction of additives but also adjustments to the type of salts, their concentration, and the solvent composition. Exploring new types of electrolytes could potentially introduce unique properties to ZIBs, including molecular crowding electrolytes, water-in-salt solutions, eutectic salts, *etc*. Reducing the content of free water within the electrolyte is a significant focus, as it can suppress water activity, effectively minimizing parasitic reactions at the electrolyte/Zn interface.

The potential for additives in practical industrial applications is considerable and deserves attention. Additives can boost battery performance by enhancing electrolyte stability, increasing ion transport efficiency, and minimizing unwanted side reactions. These improvements contribute to longer battery lifespan, higher energy density, and enhanced safety - all crucial for commercial success.

DECLARATIONS

Authors' contributions

Conceived and designed the project: Yang, S.; Zhi, C.
Wrote the main content of the paper: Yang, S.
Assisted in the writing and revision of the manuscript: Zhao, Y.; Zhi, C.
Provided useful suggestions: Zhi, C.
Contributed equally to this work: Yang, S.; Zhao, Y.
All authors discussed and commented on the manuscript.

Availability of data and materials

Not applicable.

Financial support and sponsorship

The work described in this paper was partially supported by a grant from the Research Grants Council of the Hong Kong Special Administrative Region, China (Project No. CityU C1002-21G).

Conflicts of interest

All authors declared that there are no conflicts of interest.

Ethical approval and consent to participate

Not applicable.

Consent for publication

Not applicable.

REFERENCES

1. Achakulwisut, P.; Erickson, P.; Guivarch, C.; Schaeffer, R.; Brutschin, E.; Pye, S. Global fossil fuel reduction pathways under different climate mitigation strategies and ambitions. *Nat. Commun.* **2023**, *14*, 5425. DOI PubMed PMC
2. Li, M.; Lu, J.; Chen, Z.; Amine, K. 30 years of lithium-ion batteries. *Adv. Mater.* **2018**, *30*, e1800561. DOI
3. Grey, C. P.; Hall, D. S. Prospects for lithium-ion batteries and beyond-a 2030 vision. *Nat. Commun.* **2020**, *11*, 6279. DOI PubMed PMC
4. Degen, F.; Winter, M.; Bendig, D.; Tübke, J. Energy consumption of current and future production of lithium-ion and post lithium-ion battery cells. *Nat. Energy.* **2023**, *8*, 1284-95. DOI
5. Liang, Y.; Yao, Y. Designing modern aqueous batteries. *Nat. Rev. Mater.* **2023**, *8*, 109-22. DOI
6. Ahn, H.; Kim, D.; Lee, M.; Nam, K. W. Challenges and possibilities for aqueous battery systems. *Commun. Mater.* **2023**, *4*, 367. DOI
7. Fu, Q.; Wu, X.; Luo, X.; et al. High-voltage aqueous Mg-ion batteries enabled by solvation structure reorganization. *Adv. Funct. Mater.* **2022**, *32*, 2110674. DOI
8. Li, R.; Yu, J.; Chen, F.; Su, Y.; Chan, K. C.; Xu, Z. High-power and ultrastable aqueous calcium-ion batteries enabled by small organic molecular crystal anodes. *Adv. Funct. Mater.* **2023**, *33*, 2214304. DOI
9. Liu, Y. N.; Yang, J. L.; Gu, Z. Y.; et al. Entropy-regulated cathode with low strain and constraint phase-change toward ultralong-life aqueous Al-ion batteries. *Angew. Chem. Int. Ed.* **2024**, *63*, e202316925. DOI
10. Zhang, T.; Tang, Y.; Guo, S.; et al. Fundamentals and perspectives in developing zinc-ion battery electrolytes: a comprehensive review. *Energy. Environ. Sci.* **2020**, *13*, 4625-65. DOI
11. Zhou, T.; Gao, G. V_2O_5-based cathodes for aqueous zinc ion batteries: mechanisms, preparations, modifications, and electrochemistry. *Nano. Energy.* **2024**, *127*, 109691. DOI
12. Zhang, N.; Ji, Y.; Wang, J.; Wang, P.; Zhu, Y.; Yi, T. Understanding of the charge storage mechanism of MnO_2-based aqueous zinc-ion batteries: reaction processes and regulation strategies. *J. Energy. Chem.* **2023**, *82*, 423-63. DOI
13. Li, Y.; Zhao, J.; Hu, Q.; et al. Prussian blue analogs cathodes for aqueous zinc ion batteries. *Mater. Today. Energy.* **2022**, *29*, 101095. DOI
14. Li, Z.; Tan, J.; Wang, Y.; et al. Building better aqueous Zn-organic batteries. *Energy. Environ. Sci.* **2023**, *16*, 2398-431. DOI
15. Li, C.; Wang, L.; Zhang, J.; et al. Roadmap on the protective strategies of zinc anodes in aqueous electrolyte. *Energy. Storage. Mater.* **2022**, *44*, 104-35. DOI
16. Hao, J.; Li, X.; Zeng, X.; Li, D.; Mao, J.; Guo, Z. Deeply understanding the Zn anode behaviour and corresponding improvement strategies in different aqueous Zn-based batteries. *Energy. Environ. Sci.* **2020**, *13*, 3917-49. DOI
17. Cao, J.; Zhang, D.; Zhang, X.; Zeng, Z.; Qin, J.; Huang, Y. Strategies of regulating Zn^{2+} solvation structures for dendrite-free and side reaction-suppressed zinc-ion batteries. *Energy. Environ. Sci.* **2022**, *15*, 499-528. DOI
18. Yan, C.; Xu, R.; Xiao, Y.; et al. Toward critical electrode/electrolyte interfaces in rechargeable batteries. *Adv. Funct. Mater.* **2020**, *30*, 1909887. DOI
19. Jiang, L.; Li, D.; Xie, X.; et al. Electric double layer design for Zn-based batteries. *Energy. Storage. Mater.* **2023**, *62*, 102932. DOI
20. Bockris, J. M.; Devanathan, M.; Müller, K. On the structure of charged interfaces. *Proc. R. Soc. Lond. A.* **1963**, *274*, 55-79. DOI

21. Nakamura, M.; Sato, N.; Hoshi, N.; Sakata, O. Outer helmholtz plane of the electrical double layer formed at the solid electrode-liquid interface. *Chemphyschem* **2011**, *12*, 1430-4. DOI PubMed
22. Read, J. Characterization of the lithium/oxygen organic electrolyte battery. *J. Electrochem. Soc.* **2002**, *149*, A1190. DOI
23. Ye, Z.; Cao, Z.; Lam, C. M. O.; et al. Advances in Zn-ion batteries via regulating liquid electrolyte. *Energy. Storage. Mater.* **2020**, *32*, 290-305. DOI
24. Kim, Y. P.; Shon, H. K.; Shin, S. K.; Lee, T. G. Probing nanoparticles and nanoparticle-conjugated biomolecules using time-of-flight secondary ion mass spectrometry. *Mass. Spectrom. Rev.* **2015**, *34*, 237-47. DOI PubMed
25. Yao, N.; Chen, X.; Fu, Z. H.; Zhang, Q. Applying classical, *Ab initio*, and machine-learning molecular dynamics simulations to the liquid electrolyte for rechargeable batteries. *Chem. Rev.* **2022**, *122*, 10970-1021. DOI
26. Huang, R.; Zhang, J.; Wang, W.; et al. Dual-anion chemistry synchronously regulating the solvation structure and electric double layer for durable Zn metal anodes. *Energy. Environ. Sci.* **2024**, *17*, 3179-90. DOI
27. Luo, J.; Xu, L.; Zhou, Y.; et al. Regulating the inner helmholtz plane with a high donor additive for efficient anode reversibility in aqueous Zn-ion batteries. *Angew. Chem. Int. Ed.* **2023**, *135*, e202302302. DOI
28. Chen, F. Atomistic modelling approaches to understanding the interfaces of ionic liquid electrolytes for batteries and electrochemical devices. *Curr. Opin. Electrochem.* **2022**, *35*, 101086. DOI
29. Wang, D.; Li, Q.; Zhao, Y.; et al. Insight on organic molecules in aqueous Zn-ion batteries with an emphasis on the Zn anode regulation. *Adv. Energy. Mater.* **2022**, *12*, 2102707. DOI
30. Bazant, M. Z. Theory of chemical kinetics and charge transfer based on nonequilibrium thermodynamics. *ACC. Chem. Res.* **2013**, *46*, 1144-60. DOI PubMed
31. Zheng, J.; Archer, L. A. Controlling electrochemical growth of metallic zinc electrodes: Toward affordable rechargeable energy storage systems. *Sci. Adv.* **2021**, *7*, eabe0219. DOI PubMed PMC
32. Choobar B, Hamed H, Safari M. Morphological peculiarities of the lithium electrode from the perspective of the Marcus-Hush-Chidsey model. *J. Energy. Chem.* **2023**, *80*, 452-7. DOI
33. Gileadi, E.; Eliaz, N. The mechanism of induced codeposition of Ni-W alloys. *ECS. Trans.* **2007**, *2*, 337-49. DOI
34. Santos, E.; Nazmutdinov, R.; Schmickler, W. Electron transfer at different electrode materials: metals, semiconductors, and graphene. *Curr. Opin. Electrochem.* **2020**, *19*, 106-12. DOI
35. Sato, N. Electrochemistry at metal and semiconductor electrodes. Elsevier; 1998. Available from: https://www.sciencedirect.com/book/9780444828064/electrochemistry-at-metal-and-semiconductor-electrodes [Last accessed on 9 Jan 2024]
36. Grahame, D. C. Electrode processes and the electrical double layer. *Annu. Rev. Phys. Chem.* **1955**, *6*, 337-58. DOI
37. Gileadi, E. Can an electrode reaction occur without electron transfer across the metal/solution interface? *Chem. Phys. Lett.* **2004**, *393*, 421-4. DOI
38. Bangle, R. E.; Schneider, J.; Piechota, E. J.; Troian-Gautier, L.; Meyer, G. J. Electron transfer reorganization energies in the electrode-electrolyte double layer. *J. Am. Chem. Soc.* **2020**, *142*, 674-9. DOI
39. Zhang, X.; Zhang, L.; Jia, X.; Song, W.; Liu, Y. Design strategies for aqueous zinc metal batteries with high zinc utilization: from metal anodes to anode-free structures. *Nanomicro. Lett.* **2024**, *16*, 75. DOI PubMed PMC
40. Doughty, D. H. Li ion battery abuse tolerance testing-an overview. 2006. Available from: https://www.osti.gov/servlets/purl/1725924 [Last accessed on 9 Jan 2024]
41. Dubarry, M.; Devie, A. Battery durability and reliability under electric utility grid operations: representative usage aging and calendar aging. *J. Energy. Storage.* **2018**, *18*, 185-95. DOI
42. Xiao, J. How lithium dendrites form in liquid batteries. *Science* **2019**, *366*, 426-7. DOI PubMed
43. Xu, X.; Jiao, X.; Kapitanova, O. O.; et al. Diffusion limited current density: a watershed in electrodeposition of lithium metal anode. *Adv. Energy. Mater.* **2022**, *12*, 2200244. DOI
44. Cogswell, D. A. Quantitative phase-field modeling of dendritic electrodeposition. *Phys. Rev. E. Stat. Nonlin. Soft. Matter. Phys.* **2015**, *92*, 011301. DOI PubMed
45. Li, Q.; Zhao, Y.; Mo, F.; et al. Dendrites issues and advances in Zn anode for aqueous rechargeable Zn-based batteries. *EcoMat* **2020**, *2*, e12035. DOI
46. Liu, Z.; Huang, Y.; Huang, Y.; et al. Voltage issue of aqueous rechargeable metal-ion batteries. *Chem. Soc. Rev.* **2020**, *49*, 180-232. DOI
47. Zhao, J.; Zhang, J.; Yang, W.; et al. "Water-in-deep eutectic solvent" electrolytes enable zinc metal anodes for rechargeable aqueous batteries. *Nano. Energy.* **2019**, *57*, 625-34. DOI
48. Wang, Y.; Liang, B.; Zhu, J.; et al. Manipulating electric double layer adsorption for stable solid-electrolyte interphase in 2.3 Ah Zn-pouch cells. *Angew. Chem. Int. Ed.* **2023**, *135*, e202302583. DOI
49. Liang, G.; Zhu, J.; Yan, B.; et al. Gradient fluorinated alloy to enable highly reversible Zn-metal anode chemistry. *Energy. Environ. Sci.* **2022**, *15*, 1086-96. DOI
50. Yang, Q.; Li, L.; Hussain, T.; et al. Stabilizing interface pH by N-modified graphdiyne for dendrite-free and high-rate aqueous Zn-ion batteries. *Angew. Chem. Int. Ed.* **2022**, *134*, e202112304. DOI
51. Palacín, M. R.; de Guibert, A. Why do batteries fail? *Science* **2016**, *351*, 1253292. DOI PubMed
52. Liu, B.; Yuan, X.; Li, Y. Colossal capacity loss during calendar aging of Zn battery chemistries. *ACS. Energy. Lett.* **2023**, *8*, 3820-8. DOI

53. Li, Q.; Wang, Y.; Mo, F.; et al. Calendar life of Zn batteries based on Zn anode with Zn powder/current collector structure. *Adv. Energy. Mater.* **2021**, *11*, 2003931. DOI
54. Belov, D.; Yang, M. Failure mechanism of Li-ion battery at overcharge conditions. *J. Solid. State. Electrochem.* **2008**, *12*, 885-94. DOI
55. Ji, W.; Huang, H.; Huang, X.; et al. A redox-active organic cation for safer high energy density Li-ion batteries. *J. Mater. Chem. A.* **2020**, *8*, 17156-62. DOI
56. Huang, J.; Azimi, N.; Cheng, L.; et al. An organophosphine oxide redox shuttle additive that delivers long-term overcharge protection for 4 V lithium-ion batteries. *J. Mater. Chem. A.* **2015**, *3*, 10710-4. DOI
57. Ji, W.; Huang, H.; Zheng, D.; et al. A redox-active organic cation for safer metallic lithium-based batteries. *Energy. Storage. Mater.* **2020**, *32*, 185-90. DOI PubMed PMC
58. Odom, S. A.; Ergun, S.; Poudel, P. P.; Parkin, S. R. A fast, inexpensive method for predicting overcharge performance in lithium-ion batteries. *Energy. Environ. Sci.* **2014**, *7*, 760-7. DOI
59. Ren, D.; Feng, X.; Lu, L.; He, X.; Ouyang, M. Overcharge behaviors and failure mechanism of lithium-ion batteries under different test conditions. *Appl. Energy.* **2019**, *250*, 323-32. DOI
60. Weng, W.; Huang, J.; Shkrob, I. A.; Zhang, L.; Zhang, Z. Redox shuttles with axisymmetric scaffold for overcharge protection of lithium-ion batteries. *Adv. Energy. Mater.* **2016**, *6*, 1600795. DOI
61. Wang, F.; Zhang, J.; Lu, H.; et al. Production of gas-releasing electrolyte-replenishing Ah-scale zinc metal pouch cells with aqueous gel electrolyte. *Nat. Commun.* **2023**, *14*, 4211. DOI PubMed PMC
62. Wang, F.; Tseng, J.; Liu, Z.; et al. A stimulus-responsive zinc-iodine battery with smart overcharge self-protection function. *Adv. Mater.* **2020**, *32*, e2000287. DOI
63. Li, M.; Li, Z.; Wang, X.; et al. Comprehensive understanding of the roles of water molecules in aqueous Zn-ion batteries: from electrolytes to electrode materials. *Energy. Environ. Sci.* **2021**, *14*, 3796-839. DOI
64. Yang, F.; Yuwono, J. A.; Hao, J.; et al. Understanding H_2 evolution electrochemistry to minimize solvated water impact on zinc-anode performance. *Adv. Mater.* **2022**, *34*, e2206754. DOI
65. Cao, L.; Li, D.; Hu, E.; et al. Solvation structure design for aqueous Zn metal batteries. *J. Am. Chem. Soc.* **2020**, *142*, 21404-9. DOI
66. Li, T. C.; Lim, Y.; Li, X. L.; et al. A universal additive strategy to reshape electrolyte solvation structure toward reversible Zn storage. *Adv. Energy. Mater.* **2022**, *12*, 2103231. DOI
67. Zhang, Q.; Ma, Y.; Lu, Y.; et al. Halogenated Zn^{2+} solvation structure for reversible Zn metal batteries. *J. Am. Chem. Soc.* **2022**, *144*, 18435-43. DOI
68. Zhang, Q.; Ma, Y.; Lu, Y.; et al. Designing anion-type water-free Zn^{2+} solvation structure for robust Zn metal anode. *Angew. Chem. Int. Ed.* **2021**, *60*, 23357-64. DOI
69. Jiang, L.; Zhou, Y.; Jiang, Y.; et al. Unique solvation structure induced by anionic Cl in aqueous zinc ion batteries. *Heliyon* **2024**, *10*, e30592. DOI PubMed PMC
70. Miao, L.; Wang, R.; Di, S.; et al. Aqueous electrolytes with hydrophobic organic cosolvents for stabilizing zinc metal anodes. *ACS. Nano.* **2022**, *16*, 9667-78. DOI
71. Cao, L.; Li, D.; Pollard, T.; et al. Fluorinated interphase enables reversible aqueous zinc battery chemistries. *Nat. Nanotechnol.* **2021**, *16*, 902-10. DOI
72. Li, Y.; Yu, Z.; Huang, J.; Wang, Y.; Xia, Y. Constructing solid electrolyte interphase for aqueous zinc batteries. *Angew. Chem. Int. Ed.* **2023**, *135*, e202309957. DOI
73. Li, D.; Cao, L.; Deng, T.; Liu, S.; Wang, C. Design of a solid electrolyte interphase for aqueous Zn batteries. *Angew. Chem. Int. Ed.* **2021**, *60*, 13035-41. DOI
74. Wang, G.; Zhang, Q. K.; Zhang, X. Q.; et al. Electrolyte additive for interfacial engineering of lithium and zinc metal anodes. *Adv. Energy. Mater.* **2024**, 2304557. DOI
75. Dong, Y.; Miao, L.; Ma, G.; et al. Non-concentrated aqueous electrolytes with organic solvent additives for stable zinc batteries. *Chem. Sci.* **2021**, *12*, 5843-52. DOI PubMed PMC
76. Xie, D.; Sang, Y.; Wang, D. H.; et al. ZnF_2-riched inorganic/organic hybrid SEI: in situ-chemical construction and performance-improving mechanism for aqueous zinc-ion batteries. *Angew. Chem. Int. Ed.* **2023**, *62*, e202216934. DOI
77. Chu, Y.; Zhang, S.; Wu, S.; Hu, Z.; Cui, G.; Luo, J. *In situ* built interphase with high interface energy and fast kinetics for high performance Zn metal anodes. *Energy. Environ. Sci.* **2021**, *14*, 3609-20. DOI
78. Li, Y.; Yao, H.; Liu, X.; Yang, X.; Yuan, D. Roles of electrolyte additive in Zn chemistry. *Nano. Res.* **2023**, *16*, 9179-94. DOI
79. Yao, R.; Qian, L.; Sui, Y.; et al. A versatile cation additive enabled highly reversible zinc metal anode. *Adv. Energy. Mater.* **2022**, *12*, 2102780. DOI
80. Qiu, M.; Sun, P.; Wang, Y.; Ma, L.; Zhi, C.; Mai, W. Anion-trap engineering toward remarkable crystallographic reorientation and efficient cation migration of Zn ion batteries. *Angew. Chem. Int. Ed.* **2022**, *61*, e202210979. DOI
81. Wang, H.; Ye, W.; Yin, B.; et al. Modulating cation migration and deposition with xylitol additive and oriented reconstruction of hydrogen bonds for stable zinc anodes. *Angew. Chem. Int. Ed.* **2023**, *62*, e202218872. DOI
82. Yang, Y.; Li, Y.; Zhu, Q.; Xu, B. Optimal molecular configuration of electrolyte additives enabling stabilization of zinc anodes. *Adv. Funct. Mater.* **2024**, *34*, 2316371. DOI
83. Zhao, Y.; Wei, M.; Tan, L. L.; et al. Manipulating the host-guest chemistry of cucurbituril to propel highly reversible zinc metal

anodes. *Small* **2024**, *20*, e2308164. DOI

84. Han, M. C.; Zhang, J. H.; Yu, C. Y.; et al. Constructing dynamic anode/electrolyte interfaces coupled with regulated solvation structures for long-term and highly reversible zinc metal anodes. *Angew. Chem. Int. Ed.* **2024**, *63*, e202403695. DOI
85. Dong, J.; Su, L.; Peng, H.; et al. Spontaneous molecule aggregation for nearly single-ion conducting sol electrolyte to advance aqueous zinc metal batteries: the case of tetraphenylporphyrin. *Angew. Chem. Int. Ed.* **2024**, *63*, e202401441. DOI
86. Wu, Q.; McDowell, M. T.; Qi, Y. Effect of the electric double layer (EDL) in multicomponent electrolyte reduction and solid electrolyte interphase (SEI) formation in lithium batteries. *J. Am. Chem. Soc.* **2023**, *145*, 2473-84. DOI PubMed PMC
87. Huang, C.; Zhao, X.; Hao, Y.; et al. Selection criteria for electrical double layer structure regulators enabling stable Zn metal anodes. *Energy. Environ. Sci.* **2023**, *16*, 1721-31. DOI
88. Huang, C.; Huang, F.; Zhao, X.; et al. Rational design of sulfonamide-based additive enables stable solid electrolyte interphase for reversible Zn metal anode. *Adv. Funct. Mater.* **2023**, *33*, 2210197. DOI
89. Lin, Y.; Mai, Z.; Liang, H.; Li, Y.; Yang, G.; Wang, C. Dendrite-free Zn anode enabled by anionic surfactant-induced horizontal growth for highly-stable aqueous Zn-ion pouch cells. *Energy. Environ. Sci.* **2023**, *16*, 687-97. DOI
90. Shen, Z.; Mao, J.; Yu, G.; et al. Electrocrystallization regulation enabled stacked hexagonal platelet growth toward highly reversible zinc anodes. *Angew. Chem. Int. Ed.* **2023**, *62*, e202218452. DOI
91. Ding, F.; Xu, W.; Graff, G. L.; et al. Dendrite-free lithium deposition via self-healing electrostatic shield mechanism. *J. Am. Chem. Soc.* **2013**, *135*, 4450-6. DOI
92. Ding, Y.; Zhang, X.; Wang, T.; et al. A dynamic electrostatic shielding layer toward highly reversible Zn metal anode. *Energy. Storage. Mater.* **2023**, *62*, 102949. DOI
93. Guo, X.; Zhang, Z.; Li, J.; et al. Alleviation of dendrite formation on zinc anodes via electrolyte additives. *ACS. Energy. Lett.* **2021**, *6*, 395-403. DOI
94. Xu, Y.; Zhu, J.; Feng, J.; et al. A rechargeable aqueous zinc/sodium manganese oxides battery with robust performance enabled by Na_2SO_4 electrolyte additive. *Energy. Storage. Mater.* **2021**, *38*, 299-308. DOI
95. Hu, Z.; Zhang, F.; Zhao, Y.; et al. A self-regulated electrostatic shielding layer toward dendrite-free Zn batteries. *Adv. Mater.* **2022**, *34*, e2203104. DOI
96. Wang, P.; Xie, X.; Xing, Z.; et al. Mechanistic insights of Mg^{2+}-electrolyte additive for high-energy and long-life zinc-ion hybrid capacitors. *Adv. Energy. Mater.* **2021**, *11*, 2101158. DOI
97. Jie, Z.; Xia, H.; Zhong, S. L.; et al. The gut microbiome in atherosclerotic cardiovascular disease. *Nat. Commun.* **2017**, *8*, 845. DOI
98. Kim, M.; Yun, D.; Jeon, J. Effect of a bromine complex agent on electrochemical performances of zinc electrodeposition and electrodissolution in Zinc-Bromide flow battery. *J. Power. Sources.* **2019**, *438*, 227020. DOI
99. Wang, H.; Zhou, A.; Hu, X.; et al. Bifunctional dynamic adaptive interphase reconfiguration for zinc deposition modulation and side reaction suppression in aqueous zinc ion batteries. *ACS. Nano.* **2023**, *17*, 11946-56. DOI
100. Yuan, Y.; Pu, S. D.; Pérez-Osorio, M. A.; et al. Diagnosing the electrostatic shielding mechanism for dendrite suppression in aqueous zinc batteries. *Adv. Mater.* **2024**, *36*, e2307708. DOI
101. Li, C.; Zhang, X.; Qu, G.; et al. Highly reversible Zn metal anode securing by functional electrolyte modulation. *Adv. Energy. Mater.* **2024**, *14*, 2400872. DOI
102. Zhang, N.; Cheng, F.; Liu, J.; et al. Rechargeable aqueous zinc-manganese dioxide batteries with high energy and power densities. *Nat. Commun.* **2017**, *8*, 405. DOI PubMed PMC
103. Ma, L.; Chen, S.; Li, H.; et al. Initiating a mild aqueous electrolyte Co_3O_4/Zn battery with 2.2 V-high voltage and 5000-cycle lifespan by a Co(iii) rich-electrode. *Energy. Environ. Sci.* **2018**, *11*, 2521-30. DOI
104. Liang, J.; Zhang, H.; Wan, L.; et al. Gel polymer electrolytes based on compound cationic additives for environmentally adaptive flexible zinc-air batteries with a stable electrolyte/zinc anode interface. *Energy. Storage. Mater.* **2024**, *71*, 103677. DOI
105. Wang, D.; Lv, D.; Liu, H.; et al. In situ formation of nitrogen-rich solid electrolyte interphase and simultaneous regulating solvation structures for advanced Zn metal batteries. *Angew. Chem. Int. Ed.* **2022**, *61*, e202212839. DOI
106. Huang, C.; Zhao, X.; Hao, Y.; et al. Self-healing SeO_2 additives enable zinc metal reversibility in aqueous $ZnSO_4$ electrolytes. *Adv. Funct. Mater.* **2022**, *32*, 2112091. DOI
107. Li, T. C.; Lin, C.; Luo, M.; et al. Interfacial molecule engineering for reversible Zn electrochemistry. *ACS. Energy. Lett.* **2023**, *8*, 3258-68. DOI
108. Li, J.; Zhou, S.; Chen, Y.; et al. Self-smoothing deposition behavior enabled by beneficial potential compensating for highly reversible Zn-metal anodes. *Adv. Funct. Mater.* **2023**, *33*, 2307201. DOI
109. Wan, J.; Wang, R.; Liu, Z.; et al. A double-functional additive containing nucleophilic groups for high-performance Zn-ion batteries. *ACS. Nano.* **2023**, *17*, 1610-21. DOI
110. Bai, X.; Nan, Y.; Yang, K.; et al. Zn ionophores to suppress hydrogen evolution and promote uniform Zn deposition in aqueous Zn batteries. *Adv. Funct. Mater.* **2023**, *33*, 2307595. DOI
111. Wang, Y.; Wang, Z.; Pang, W. K.; et al. Solvent control of water O-H bonds for highly reversible zinc ion batteries. *Nat. Commun.* **2023**, *14*, 2720. DOI PubMed PMC
112. Dong, Y.; Zhang, N.; Wang, Z.; et al. Cell-nucleus structured electrolyte for low-temperature aqueous zinc batteries. *J. Energy. Chem.* **2023**, *83*, 324-32. DOI